

CONSIDERATION ON THE DENSITY EVALUATION OF THE MODEL OF HEAVY HYDROCARBONS BY COMPUTER SIMULATION

Masakatsu NOMURA, Satoru MURATA, Koh KIDENA, Takenao OOKAWA* and Hisanori KOMODA*

Department of Molecular Chemistry, Graduate School of Engineering, Osaka University; *Department of Information Systems Engineering, Graduate School of Information Science and Technology, Osaka University
2-1 Yamada-oka, Suita, Osaka 565-0871 Japan

Introduction

The authors have been studying the modeling of molecular structure of heavy hydrocarbons such as coal and petroleum derived asphaltene because these heavy hydrocarbons have a very complicated mixture of relatively higher molecular weight hydrocarbons. In order to convert these materials into more useful smaller molecular weight fractions it is believed indispensable to know the chemical structures of these materials at molecular level. For this purposed measurements of molecular weight of original substances, identification of the bridge bonds of aromatic clusters and quantitative analysis of carbon functionalities of heavy hydrocarbons are considered indispensable. Molecular weight distribution of a complicated mixture of hydrocarbons is now determined by the use of MALDI although the more heavy portions due to association structure can not be detected even by this method. As for the bridge bonds connecting aromatic nuclei which are thought to govern the reactivity of heavy hydrocarbons has been studied by many researchers, however, for coal Stock[1] applied ruthenium ion catalyzed oxidation reaction to clarify these chemical structures and Strausz[2] undertook the same reaction for asphaltene derived from oil sand bitumen. Both groups published the model structures based on these results in 1993 and 1992, respectively. As for the quantitative analysis of carbon functionalities, Snape[3] published the successful application of ^{13}C NMR spectroscopy with single pulse excitation MAS method. Using these data available so far the authors published the model structures of Zao Zhuang coal[4] and Arabian light/medium vacuum residue derived asphaltene[5] in 1998 and 1999, respectively.

However, in spite of these continuing efforts of many researchers, there are few means to examine the comprehensiveness of the model structures. One seems to be the estimation of density of proposed model structures using computer simulation method, however, which needed an expensive software and high-performance calculator at the beginning of 1990's. Right now such calculation can be easily attained due to the rapid growth of computer science. Recently several researchers still are proposing model structures of these heavy hydrocarbons without knowing the spacious arrangement of these chemical structures.[6] This is the reason why the authors are going to present this article.

Experimental

Estimation of the physical density of model molecule was performed with CAMD (computer-aided molecular design) software, which is running on Polygraf (ver.3.0, Molecular simulations Inc.). Detail of the procedure was shown elsewhere[7], but it would be

shown here briefly. At first, the model molecule was input, and its potential energy was then optimized. The conformation having the lowest potential energy was extracted as a best conformer. This model molecule was enclosed in cell, periodic boundary condition. For this PBC calculation, hydrogen atoms attached to carbon or oxygen atoms were treated as included in each carbon or oxygen group such as methane, methylene, methyl or hydroxyl group according to DREIDING's method. Molecular mechanics calculation was then carried out in order to reduce the potential energy of the system up to its minimum value, by using a cell volume of which the true density can be calculated.

Results and Discussion

Calculation of density of the model structure of oil sand bitumen derived asphaltene by Strausz *et al.*[2] Figure 1 shows the structure of asphaltene proposed by Strausz *et al.* This structure has the molecular formula of $\text{C}_{410}\text{H}_{817}\text{N}_5\text{O}_2\text{S}_{13}$ with molecular weight of 5950.1. The structural features of this model are the presence of porphyrine moiety and a relatively large loop structure with two small loop structures. The authors have applied their own method to calculate the density to get the value of 0.98 g/cm^3 . According to the reported value of this asphaltene's density, 1.2 g/cm^3 the loose packing due to the presence of above mentioned structural portions is considered as the reason for such a very low density value. The authors have succeeded in getting reasonable value of density such as 1.17 g/cm^3 by rearranging two molecules from the original structure by cutting two bridge bonds shown in Figure 1. The resulting structure has still small loop structures in it, however, the presence of these loops shows little effect for the reasonable value of the density. This consideration should be examined. Incidentally, in the previous paper about coal structure that was published in 1992 by one of the author, the model structure had loop structure. It was considered to represent the average size of the void that could be measured experimentally for the sample. The asphaltene structure by Strausz *et al.* had several loop structures which probably were assumed to represent the presence of void structures in the asphaltene sample.

Calculation of the density of Arabian light/medium vacuum residue derived asphaltene model structure by Nomura *et al.*[5] The model structure is shown in Figure 2 where the model has molecular formula of $\text{C}_{490}\text{H}_{528}\text{N}_4\text{O}_5\text{S}_{15}$ with molecular weight 7034.5. This model is constructed based on the results from RICO reaction results and measurements of ^{13}C NMR spectrum and solid proton NMR spectroscopy. According to the measurement of molecular weight of this fraction using gel permeation chromatography the use of chloroform eluent gave relatively higher molecular weight while the use of more polar tetrahydrofuran eluent made the maximum peak of the molecular weight of the fraction to the relatively lower molecular weight. From the Figure 2, this asphaltene fraction consists of four portions and each portion can associate each other. This feature seems to be natural according to the current studies on these heavy hydrocarbons. The calculation was conducted to give 1.06 g/cm^3 of its density, this value being close to the observed value of 1.16 g/cm^3 . In fact the real structure has more than thousand compounds in it so that the authors are thinking to take two phase models into consideration because in this asphaltene the relatively smaller fraction can be contained to exert a little effect on the calculation of the density of this fraction.

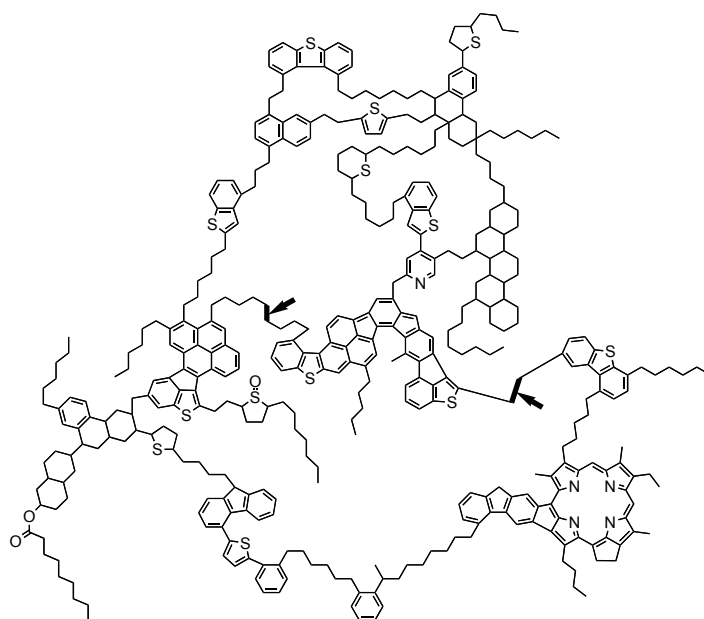


Figure 1. Hypothetical asphaltene molecule proposed by Strausz *et al.* (reference 2) Bold line and arrows in the figure indicate the position of cutting bridges in order to rearrange the three-dimensional structure of the molecule.

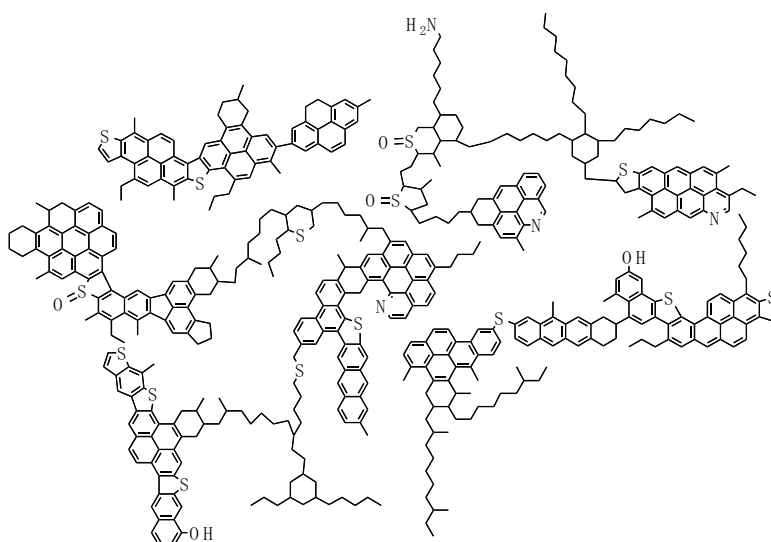


Figure 2. A model molecule for Arabian light/medium vacuum residue derived asphaltene proposed by Nomura *et al.* (reference 5)

Summary

This paper considers over again about the density evaluation with computer simulation method. One model structure was proposed by Strausz *et al.* that had a moiety of porphyrin and several loops. The other model was ours.

Acknowledgement. This work has been carried out as a research project of The Japan Petroleum Institute commissioned by The Petroleum Energy Center with the subsidy of The Ministry of International Trade and Industry.

References

- (1) Stock, L. M.; Muntean J. V. *Energy Fuels*, **1993**, *7*, 704.
- (2) Strausz, O. P.; Mojelsky, T. W.; Lown, E. M. *Fuel*, **1992**, *71*, 1355.
- (3) Franz, J. A.; Garcia, R.; Linehan, J. C.; Love, G D.; Snape, C. E. *Energy Fuels*, **1992**, *6*, 598.
- (4) Nomura, M.; Artok, L.; Murata, S.; Yamamoto, A.; Hama, H.; Gao, H.; Kidena K. *Energy Fuels*, **1998**, *12*, 512.
- (5) Artok, L.; Su, Y.; Hirose, Y.; Hosokawa, M.; Murata, S.; Nomura, M. *Energy Fuels*, **1999**, *13*, 287.
- (6) Mathews, J. P.; Hatcher, P. G.; Scaroni, A. W. *Energy Fuels*, **2001**, *15*, 863.
- (7) Nakamura, K.; Murata, S.; Nomura, M. *Energy Fuels*, **1993**, *7*, 347.

CHARACTERIZATION OF CONSTITUENTS OF ARABIAN VACUUM RESIDUES BY FT-ICR MS COUPLED WITH VARIOUS IONIZATION TECHNIQUES

Keiko Miyabayashi, Yasuhide Naito, Kazuo Tsujimoto,
Mikio Miyake

School of Materials Science,
Japan Advanced Institute of Science and Technology (JAIST)
1-1 Asahidai, Tatsunokuchi,
Ishikawa 923-1292 Japan

Introduction

Fourier transform ion cyclotron resonance (FT-ICR) mass spectrometry provides ultrahigh resolution spectra with exact mass of more than 6 orders magnitudes. Such novel performance causes us to investigate potential application of FT-ICR mass spectrometry to determine molecular formula of constituents in vacuum residues directly without any pre-separation procedures. Electrospray ionization (ESI) is promising technique to ionize non-volatile compounds without fragmentation. In our previous report, we have demonstrated effectiveness of ESI FT-ICR mass spectrometry to estimate molecular formulas of constituents in Arabian vacuum residues.¹ Recent our results suggest that aromatic compounds with more than 4 condensed rings are ionized under adopted ESI conditions. On the other hand, electro ionization (EI) proved to ionize aliphatic compounds in vacuum residues.² Therefore, selection of ionization is very important to analyze specific types as well as variety of compounds in vacuum residues.

In the present study, liquid secondary ionization (LSI) is applied to analyze vacuum residues, which is known to have extensive ionization ability irrespective of polar and apolar compounds. The results obtained by three different ionization systems are discussed to characterize features of respective ionization methods.

Experimental

Vacuum Residue Samples. The sample used in this study is Arabian vacuum residue with elemental composition (wt%) of C 84.3, H 9.9, S 5.2, N 0.4, and O 0.2 (diff.). The ESI and LSI were applied to whole the sample without any separation procedures, while the fraction eluted by *n*-heptane was used for EI.^{1,2} HPLC grade methanol and chloroform were used without further purification. All the other solvents and reagents were at least guaranteed reagent grade obtained from Wako Pure Chemical Industries, Ltd.

Ionization Conditions. For LSIMS measurement, the vacuum residue sample was mixed with 3-nitrobenzylalcohol used as a liquid matrix. Approximately 1 μ l of the liquid slurry was directly loaded on the probe tip. The primary ion (Cs^+) gun was operated at anode potential of 10 kV. The extraction voltage in the source was 10 V and the ionization pulse length was set to 600 ms.

For EI measurement, the sample dissolved in methylene chloride was loaded on the In-beam EI probe tip. The optimum conditions of probe temperature and ionization energy were estimated to be 300 °C and 30 eV, respectively in a previous study² and adopted in the present study.

The sample dissolved in methanol/chloroform (0.8/0.2, v/v) were infused into the ESI source in a positive ion mode and were desolvated by countercurrent nitrogen gas heated at 250 °C. Nitrogen needle-gas was flowed from the grounded needle to metal-capped glass capillary (~ -3.5 kV). Ions were accumulated in the hexapole for 3s before transporting to the FT-ICR cell. Detailed procedures were described previously.¹

Mass Spectrometry. All spectra were accumulated by

BioAPEX 70e with an external ion source. A broad band chirp excitation was used for all the experiments. Molecular formulas (possible combination of atomic masses which give the least deviation from the measured mass) were obtained by using *mass analysis* module. ESI and SIMS FT-ICR mass spectra were internally calibrated by using (poly)-ethylene glycol with the average molecular weight of 300 and/or 600. EI FT-ICR mass spectra were internally calibrated by using perfluorotributylamine. Detailed conditions are similar to those reported previously.^{1,2}

Results and Discussion

FT-ICR mass spectra obtained by using LSI (a), EI (b), and ESI (c) are shown in **Figure 1**. Over 500 distinguishable peaks originating from components of Arabian vacuum residues were observed for every spectrum. An order of ionization methods to detect higher masses were as follows: ESI (~ 800 Da) > EI (~ 600 Da) > LSI (~ 450 Da). It should be mentioned that heavier fraction in vacuum residue is eliminated for EI sample. The low acceleration voltage of primary ion (10 kV) adopted for LSI may be responsible for the low upper mass limit. The peaks with small masses detected by LSI should originate from molecular ions because LSI is known to be one of the soft ionization techniques by the aid of matrix and the low acceleration voltage was adopted in the present study. On the other hand, such peaks with low molecules are mostly olefins, resulting from fragmented ions of alkyl side-chains.² Adoption of the higher acceleration voltage is expected to detect molecules with the higher masses by LSI.

The expanded mass spectra show significant difference in peak positions and patterns depending on ionization methods (**Figure 1** insets). The difference in peak positions should be caused by the detection of compounds with different kinds of hetero-atoms, number of double bonds, or number of rings. When focused on patterns of a sequence of adjacent peaks appeared in ESI spectrum, abundance of peaks with even masses was observed compared to those with odd masses, compatible with the detection of compounds with monoisotopic and ¹³C isotopic ions, respectively. On the other hand,

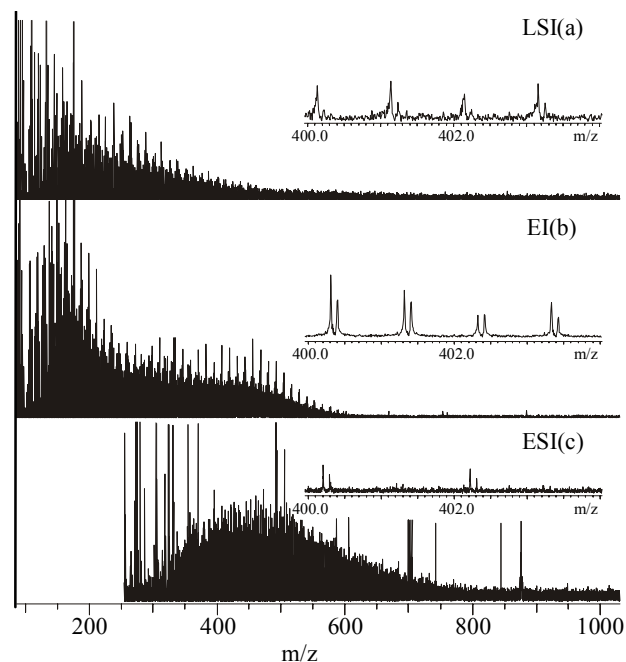


Figure 1. FT-ICR mass spectra of Arabian vacuum residue in each ionization technique; LSI(a), EI(b), and ESI(c). Insets show mass scale expansion from 400 to 404 Da.

Table 1. Estimated Molecular Formulas for the Peaks m/z 271.1503, 272.1426, 274.1588, 275.0900 and 275.1796 in Fig. 1(a)

Measd. mass / Da	Molecular formula	Formula mass / Da (Difference / mDa)	Z*
271.1503	$[C_{18}H_{22}S+H]^+$	271.1515 (0.8)	-14
272.1426	$[C_{20}H_{17}N+H]^+$	272.1434 (-0.8)	-23
274.1588	$[C_{20}H_{19}N+H]^+$	274.1590 (0.2)	-21
275.0900	$[C_{19}H_{15}S+H]^+$	275.0889 (1.1)	-23
275.1796	$[C_{21}H_{22}+H]^+$	275.1794 (0.2)	-20

*Hydrogen deficiency index: $[C_nH_{2n+Z}N_mS_s+H]^+$

adjacent peak intensities were random for EI spectrum, due to existence of the molecular ions (even mass) and fragment ions (odd mass) simultaneously.² LSI showed similar peak patterns to those of EI. Odd-mass ions detected in LSI may correspond to the compounds with zero or even-numbers of nitrogens based on soft ionization conditions. In every mass spectrum, a clear periodicity appears with similar peak intensities repeating at every 14 nominal mass unit. This periodicity predicts the presence of a series of compounds with different methylene chains. These homologues were detected irrespective of compound species, since the detected components changed by ionization. The chemical formulas of compounds detected by LSI were characterized on the basis of accurate mass measurements. The most plausible molecular formulas estimated for the measured peaks of $271 < m/z < 275$ are shown in Table 1, together with hydrogen deficiency index denoted by $C_nH_{2n+Z}X$. The deviation between measured and calculated masses is very small; less than 1.1 mDa. Hydrocarbons, S-containing compounds, and N-containing compounds ($[C_nH_{2n+Z}+H]^+$, $[C_nH_{2n+Z}S+H]^+$, and

$[C_nH_{2n+Z}N+H]^+$, respectively) are detected as major peaks in the LSI mass spectrum ($230 < m/z < 330$), whose distributions are summarized in Figure 2.

The most abundant constituents were S-containing compounds with carbon and Z number of 17~18 and -18~-22, respectively. Considerable difference in compound type distribution was observed for hydrocarbons, S-containing and N-containing compounds. Furthermore, we observe significant difference in peak intensities for kinds and types of compounds among three ionization techniques. For example, hydrocarbons and S-containing compounds were detected in similar intensities by EI, whereas N-containing compounds were detected preferentially by ESI.

The ranges of detected carbon numbers and hydrogen deficiency indexes for each ionization technique were summarized for comparison in Table 2. Hydrocarbons and S-containing compounds with similar carbon numbers are detected by EI and LSI, while whose hydrogen deficiency indexes by LSI is smaller than those by EI. Thus, it is anticipated that paraffinic and highly aromatic compounds are preferentially ionized by EI and LSI, respectively. N-containing compounds were detected both by ESI and LSI. Therefore, it is demonstrated that the detectable compounds vary depending on an ionization technique; each of them complements the analysis of complex mixture.

Table 2. Detectable Constituents of Arabian Vacuum Residue in EI, ESI, and LSI Mass Spectrometry.

	EI	ESI	LSIMS
C-number	7 ~ 30 (C_nH_{2n+Z})		12 ~ 22 (C_nH_{2n+Z})
	8 ~ 27 ($C_nH_{2n+Z}S$)		11 ~ 30 ($C_nH_{2n+Z}S$)
		27 ~ 59 ($C_nH_{2n+Z}N$)	12 ~ 33 ($C_nH_{2n+Z}N$)
Z-number	-16 ~ 2 (C_nH_{2n+Z})		-24 ~ -12 (C_nH_{2n+Z})
	-14 ~ -4 ($C_nH_{2n+Z}S$)		-26 ~ -14 ($C_nH_{2n+Z}S$)
		-46 ~ -8 ($C_nH_{2n+Z}N$)	-32 ~ -14 ($C_nH_{2n+Z}N$)

References

- (1) Miyabayashi, K.; Suzuki, K.; Teranishi, T.; Naito, Y.; Tsujimoto, K.; and Miyake, M. *Chem. Lett.*, **2000**, 172.
- (2) Miyabayashi, K.; Naito, Y.; Tsujimoto, K.; and Miyake, M. *Int. J. Mass. Spectrom.* **2002**, 221, 93.

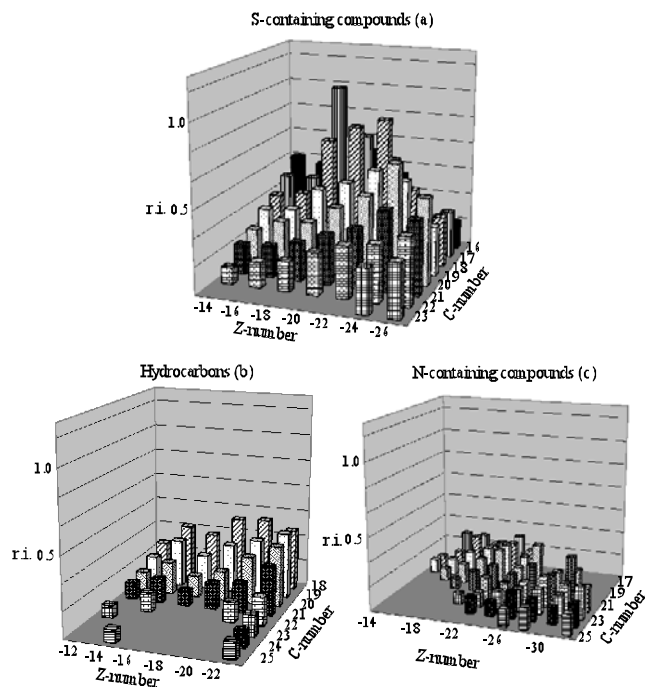


Figure 2. The Compounds distribution detected in LSI mass spectrum; (a) S-containing compounds, (b) Hydrocarbons, and N-containing compounds(c).

VAPOR LIQUID EQUILIBRIUM IN POLYCYCLIC AROMATIC COMPOUND MIXTURES AND IN COAL TARS

Vahur Oja and Eric M. Suuberg

Division of Engineering, Brown University, Providence, RI 02912, USA (Eric_Suuberg@brown.edu)

Introduction

There exist very few data in the literature concerning the vapor-liquid equilibrium (VLE) behavior of mixtures of high molecular weight organics. This is because it is difficult to measure the vapor pressures of high molecular weight organics without their undergoing thermal degradation during measurement. The present study addresses the problem, by presenting some new data on mixtures of polycyclic aromatic compounds (PAC) and mixtures of PAC with coal tar. The data were obtained by using the Knudsen effusion method, which avoids the degradation problem. The main focus of the present study is the question of whether high molecular weight PAC mixtures can be regarded as "ideal", and therefore, whether Raoult's law can describe their VLE behavior.

Experimental

Vapor pressures were indirectly determined, using the implementation of the Knudsen effusion method published earlier [1]. Briefly, this method involves the measurement of the rate of effusion of a compound (or mixture components) through a pinhole leak in a capsule that is suspended from one arm of a continuously recording microbalance. These results are readily related to vapor pressures. The measurements were conducted in a high vacuum ($<10^{-7}$ torr), which permitted measurements of vapor pressure to as low as 10^{-6} torr. Because of the low vapor pressures that can be measured, the temperatures of measurement can be kept sufficiently low so as to prevent significant thermal degradation of the sample during the measurement.

The PAC materials examined here were pure (reagent grade or best available purity) materials, and were used as received with no further purification. The materials were in all cases of 98+% purity. Preparation of mixtures of PAC was accomplished using the so-called "quenching" method. This method involved measuring the desired amounts of two PAC compounds into a stainless steel capsule, under inert gas. After closing, the capsule was shaken, while the contents were heated to melting. "Instant" cooling was achieved by plunging the capsule into liquid nitrogen. It was assumed that this method provided "perfect" mixing of the components. No visible phase separation was observed in the samples prepared in this manner. It is fair to note that questions have been raised regarding the efficacy of this method, for preparing truly homogeneous crystalline mixtures [3]. This will be considered further below.

The coal tar was prepared from a sample of Illinois No. 6 coal, obtained from the Argonne Premium Coal Sample Program [2]. The tar was prepared by pyrolysis of the coal in a tube furnace, in inert gas at 700°C, and collected by washing the cold end of the reactor (at which the tars condensed) using tetrahydrofuran (THF). The THF solvent was fully removed from the tar sample by vacuum drying at 45°C. This procedure allowed capture of the tars with molecular weight greater than 150 daltons. Following preparation, the tar was separated on a preparative-scale gel permeation chromatography (GPC) column, using two styrene-divinylbenzene GPC columns in series. The separation solvent was THF. The separation was not a pure size separation, but depended somewhat on molecular

properties. This is not important in the present work. The number average molecular weight of the tar was determined by vapor phase osmometry (VPO), in pyridine. The separated tar fraction was dried in vacuum at 50°C, to fully remove the THF solvent.

Results and Discussion

Figure 1 shows results typical of those obtained in this study. The results are for an equimolar mixture of anthracene (MP=491 K) and perylene (MP=551 K). As might be concluded from the above melting points, results in Figure 1 are, strictly speaking, for sublimation of the compounds. The predicted behavior, assuming that Raoult's Law is followed, is also shown in Figure 1. The calculation of the mixture vapor pressure in this case is assumed to follow:

$$P = x_1P_1^0 + x_2P_2^0$$

In which the x_i represent the component mole fractions and the P_i^0 represent the respective pure component vapor pressures. These pure component vapor pressures were determined as part of this study, and were generally in excellent agreement with values found in the literature [4].

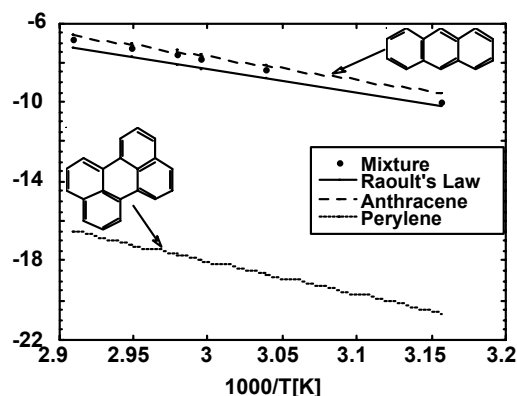


Figure 1. Vapor pressures of an equimolar mixture of anthracene and perylene.

While these data seem to suggest that Raoult's Law behavior might represent a fair approximation of the behavior, it is difficult to make a firm judgment of this, insofar as the disparity in pure component vapor pressures is so large that the lower molecular weight component (anthracene) dominates the behavior. On the other hand, Figure 2 shows that in a mixture of anthracene and benzofluorene, Raoult's Law is clearly not followed. This figure presents clear evidence of mixture non-ideality. The result might have been anticipated, since the mixture was below the melting point. Even though to the eye, the mixture appeared homogeneous, it could well have been phase separated. In such a case, the two solid phases behave as thermodynamically separate entities, as far as the vapor pressures they exert. The tendency to approach Raoult's Law behavior at higher temperatures was observed here and in several other cases. This suggests that as the systems approach melting they begin to behave as more nearly ideal single phases.

What is important to note from Figure 2 is the direction of deviations from Raoult's Law. If two phases behave independently of one another, their combined vapor pressure is

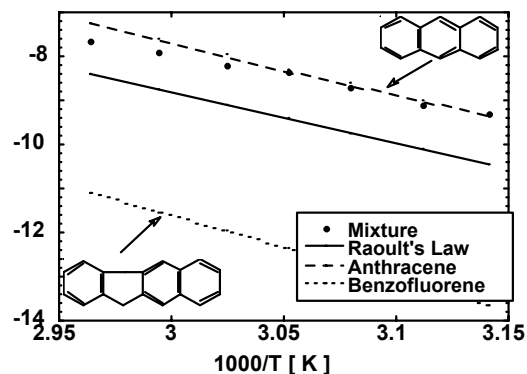


Figure 2. Vapor pressure behavior of a mixture of 25 mol % anthracene and 75mol % bezofluorene.

essentially the summation of the individual vapor pressures. Keeping this in mind, the contrasting results of Figure 3, for a mixture of 1-hydroxypyrene and phenanthridine are considered. In this instance, the mixture deviates in a direction of lower vapor pressure than the Raoult's Law prediction. This behavior cannot be explained by the possibility of phase separation. Rather, there is here strong evidence of a molecular interaction between the mixture partners. This could have perhaps been anticipated in light of the nitrogen base character of the phenanthridine and the acid (phenolic) nature of the 1-hydroxypyrene.

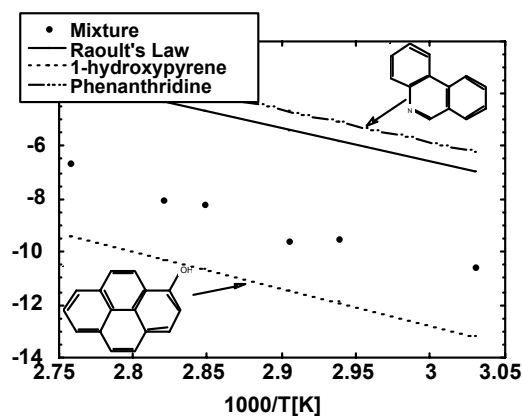


Figure 3. Vapor pressure behavior of a mixture of 54 mol% 1-hydroxypyrene and 46 mol% phenanthridine.

With these pure component and mixture results as a guide, the phase behavior of mixtures of PAC with coal tars was examined. A fraction of Illinois coal tar with a number average molecular weight of 270 daltons was mixed with pure compounds of similar molecular weight. It was estimated from elemental analysis that each "average" molecule of the tar contained about two hydroxyl groups, and the hydroxyl-rich character of this fraction was supported by its elution behavior in the GPC (its elution time was consistent with that of OH-rich species). The elemental analysis of this fraction showed that, by comparison, only every fifth tar molecule could contain nitrogen.

Figure 4 displays the VLE behavior of a mixture of the Illinois coal tar and 1-hydroxypyrene.

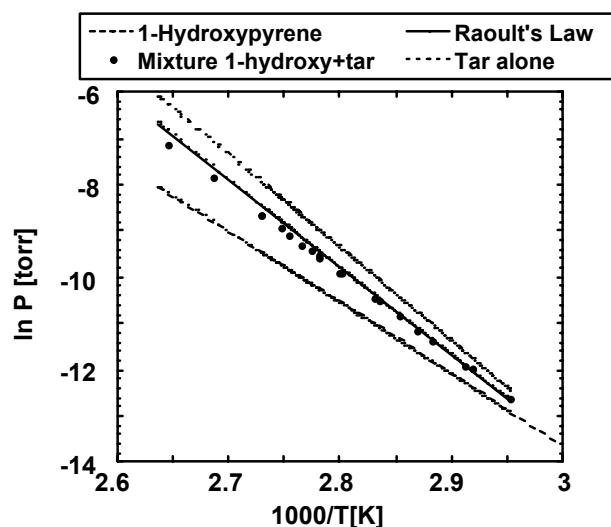


Figure 4. Vapor pressure behavior of 50 mol% 1-hydroxypyrene with 50 mol% Illinois No. 6 coal tar.

It is observed that the mixture of a phenolic compound with the coal tar produces what is very close to ideal mixture behavior. This is because the chemical nature of both components of the mixture is quite similar. On the other hand, addition of phenanthridine to the coal tar produces a mixture (Figure 5) that shows a significantly lower vapor pressure than predicted by Raoult's Law, and consistent with the behavior observed in Figure 3. This shows that the behavior of nitrogen compounds in the coal tar mixtures cannot be assumed to necessarily follow ideal mixture rules.

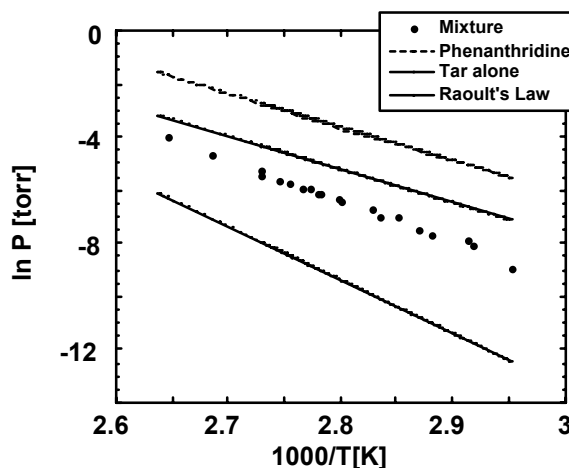


Figure 5. Vapor pressure behavior of phenanthridine (35 mol %), and Illinois coal tar (65 mol%).

Reference:

- (1) Oja, V.; Suuberg, E.M. *Anal. Chem.*, **1997**, *69* 4619.
- (2) Vorres, K. *Energy and Fuels*, **1990**, *4*, 420.
- (3) DeKruif, C.G.; van Genderen, C.G.; Bink, J.C.W.; Oonk, H.A. J., *J. Chem. Thermodyn.*, **1981**, *13*, 1081.
- (4) Oja, V.; Suuberg, E.M. *Jl of Chem. Eng. Data*, **1998**, *43*, 486.

UPGRADING OF HAMACA CRUDE OIL USING FORMIC ACID AS HYDROGEN PRECURSOR UNDER STEAM INJECTION CONDITIONS.

^{1,3}Scott C. E., ¹Delgado O., ¹Bolívar C., and ²Ovalles C.

¹ Centro de Catálisis Petróleo y Petroquímica, Facultad de Ciencias, Universidad Central de Venezuela, Apartado Postal 47102, Los Chaguaramos, Caracas 1042A, Venezuela.

² PDVSA Intevep, Departamento de Exploración y Producción, Sector El Tambor, Los Teques, Estado Miranda, Venezuela.

³ Corresponding author: cscott@strix.ciens.ucv.ve

Introduction

Heavy and extra-heavy crude are found in vast abundance in different places, thus, for instance the heavy oil and tar sands bitumen in Alberta Providence of Canada and in the Orinoco Belt of Venezuela are each as large as the oil deposits in Saudi Arabia[1]. However, there are tremendous disadvantages in the recovery, transportation and refining of heavy crude oils because their densities and viscosities are much higher than the conventional ones. The use of downhole upgrading has been proposed in order to enhance heavy crude oil recovery. Several methods, as deasphalting[2-5], visbreaking[6-9] underground hydrogen[10-17] or *in situ* combustion[18-20], as well as hydrogen donor solvents[21-23] have been proposed as possible enhanced recovery technologies. Also, the injection of hydrogen precursors downhole has been reported as a way of *in situ* partially upgrading heavy crude oils. In fact, a 1992 patent[24] claims that *in situ* hydrogenation in a subterranean formation is readily performed by introducing a non gaseous hydrogen precursor into the oil bearing subterranean formation to enhance oil recovery. Formic acid and its organic and inorganic salts are among the hydrogen precursors proposed in the patent. It is reported that after treating a crude oil in a batch reactor with formic acid and MoS₂ (as catalysts), at 573 K and 1600 psig, API gravity of the upgraded oil is increased and asphaltene content is reduced, however, a detailed characterization of the upgraded product is not given.

In this work, a detailed study of the effect of formic acid in the upgrading of Hamaca extra-heavy oil, under steam injection conditions, was carried out. Laboratory physical simulations, using a batch reactor, at 553 K and 1500-1600 psig will be presented. The reactor was fed with a mixture of crude oil and sand (99 w % SiO₂) having 10 wt % crude oil, together with formic acid, and water. We believe that this conditions more closely represent the actual situation found during crude oil recovery by steam stimulation processes.

Experimental

Upgrading reactions were performed in a stainless-steel 300 cm³ batch reactor (Parr), without stirring. In a typical test, the reactor was fed with 55 g. of Hamaca crude oil and sand (silboca, 99 w % SiO₂, specific area < 1 m² g⁻¹) containing 10 % by weight of oil, 5 g. of formic acid and 5g. of distilled water. Experiments with no water added were also carried out. The reactor was heated at 4.2 K min⁻¹, to 553 K. Prior to heating the system was purged with nitrogen and pressurized up to 500 psig. Final pressure, after heating, was around 1300 psig (for experiments without Formic Acid) and 1600 psig (for experiments with Formic Acid). All the reactions were carried out for 24 hours. The reactor was then allowed to cool down to room temperature and the upgraded oil was removed from sand by solvent extraction with dichloromethane.

Original Hamaca and Extracted oils were analyzed for sulfur, using an ANTEK sulphur analyzer. Saturated, Aromatics Resins and Asphaltene (SARA) separation and quantification were done in a

Iatroscan MK-5 on samples separated on thin layer chromatography and detected by a hydrogen flame ionization system.

Results and Discussion

SARA analysis are presented in Table 1. It is found that treating the Hamaca crude oil in presence of water (W) produces a decrease in the Asphaltene and Resins (13.9 and 35.5 % conversions respectively), with the corresponding increase in the Aromatics and Saturates fractions. This is in agreement with previous reports[25] in which a reduction of the Asphaltenes and Resins fractions, and the corresponding increase of Aromatics and Saturates ones is found after treating heavy crude oils in the presence of steam.

When the crude oil is treated in presence of formic acid (FA), a slightly higher degree of Asphaltene conversion is obtained (23.1 %), while resins are converted to a lesser extend (22.2%). Again Aromatics increase, but in this case, Saturates are close to its content in the original oil. When formic acid was used in conjunction with water (FA+W) best results are obtained. Thus, Asphaltenes are reduced in 29.2 % and Resins in 44.5 %. Obviously, formic acid is more efficient in upgrading the oil when used together with water.

Table 1. SARA Fractions for Untreated and Upgraded Hamaca Crude Oil.^a

	Saturates/ wt %	Aromatics/ wt %	Resins/ wt %	Asphaltenes/ wt %
HAMACA	(8.0 ± 0,8)	(34 ± 4)	(45 ± 2)	(13 ± 1)
W	(11.9 ± 0,6)	(48 ± 2)	(29 ± 1)	(11.2 ± 0.6)
FA	(7 ± 1)	(51 ± 1)	(32 ± 1)	(10 ± 1)
FA+W	(10.4 ± 0,5)	(55 ± 3)	(25 ± 1)	(9.2 ± 0.5)

^a Reactions carried backwise, no stirring, at 1600 psi and 553 K for 24 h. Ratio solid: crude oil: formic acid: water = 10:1:1:1.

Sulfur content on the Hamaca crude oil, before a after upgrading was also measured, and the results are presented in Table 2. For the crude oil treated in presence of water a sulfur reduction of 20 %, is observed, which is due to thermal desulfurization[25]. When formic acid alone is used, the percentage of desulfurization is less (only 12%), but when formic acid and water are used together, the desulfurization is increased to 38 %, which is an important amount if we take into account that this is intended to be a downhole process.

All the results (SARA and sulfur content) presented show that an important degree of upgrading is obtained when Hamaca crude oil is treated in very mild conditions, i.e. conditions that are normally used in the reservoir during steam injection, using formic acid to generate hydrogen in the reaction media. The upgrading is more important when formic acid is used together with water.

Formic acid thermal decomposition have been proposed to proceed by two different basic mechanisms [26,27]



It has been found that major products are CO₂ and H₂, for conversions between 38 to 100 %, temperatures of 593-773 K and pressures in the range of 2600-4500 psia. These conditions are similar to the ones used in this work, so it can be assumed that in the upgrading reactions conditions used in this work the main decomposition path way is the decarboxilation (reaction 2). In fact, molecular H₂ and CO₂ were observed in high proportions in the gaseous products, with only small amounts of CO. On the other hand, thermodynamic calculations[23] have shown that during the

hydrothermal decomposition of formic acid water acts as a catalyst, by forming an intermediate between a water dimmer and formic acid. It is suggested that Formic Acid and the water dimmer are bound with two hydrogen bodings and that the water dimmer acts simultaneously as a proton donor and acceptor. This configuration greatly reduces activation energy of the decomposition process.

Table 2. Sulfur content for original and upgraded oil. ^a

	(S ± 0.06)/ %	Desulfurization/ %
HAMACA	3.79	-
W	3.02	20
FA	3.34	12
FA+W	2.36	38

^a Same conditions as for Table 1.

The results here presented show the potential of formic acid when used together with water, for giving up H₂ in steam injection conditions. H₂ produced in this way is effectively used for upgrading Hamaca crude oil disperse in sand. In the process water acts as a catalysts for the thermal decomposition of the formic acid.

Conclusions

H₂ produced by decomposition of formic acid can be effectively used for upgrading Hamaca crude oil disperse in sand at mild conditions (553 K, 1500 to 1600 psig of N₂). When formic acid is used in conjunction with water, water acts as a catalysts for the thermal decomposition of the formic acid, and the oil is upgraded to a higher extend. Thus, for Hamaca oil upgraded in the presence of formic acid and water, a 29 % conversion of asphaltene, and 38 % of desulfurization are obtained.

Acknowledgement. The authors are grateful to FONACYT (CONICIT-CONIPET 97003783) for financial support. Also the assistance from Laboratorio de Fisicoquímica de Hidrocarburos of the UCV in the SARA analyses is gratefully acknowledged.

References

- Wiehe, I. A., *Am. Chem. Soc., Div. Pet. Chem. Prepr.* **2001**, 46 (1), 60.
- US Patent 3 608 638, **1971**.
- US Patent 4 753 293, **1988**.
- Butler, R. M. and Mokry, I. J. SPE 25425, presented in Productions Operations Symposium, Oklahoma City, USA, March 21-23, **1993**.
- Duerksen, J. H. and Eloyan, A. M. Proceeding 6th UNITAR Int. Conf. On Heavy Crude and Tar Sands, Houston, Texas, USA, Feb 12-17, 1995, 353.
- Henderson, J. H. and Weber, L. *J. Can. Pet. Tech.*, Oct-Dec, **1965**, 206.
- Kasrale, M. and Faroug, A. SPE 18784 presented in SPE California Regional Meeting, Bakersfield, USA, April 5-7, **1989**, 389.
- Shu, W. R. and Hartman, K.J. *SPE Reserv. Eng.* **1986** (September), 474.
- Monin, J. C. and Audibert, A. *SPE Reserv. Eng.* **1988** (Nov), 1243.
- US Patent 3 208 514, **1965**.
- US Patent 4 050 515, **1977**.
- US Patent 4 444 257, **1984**.
- US Patent 4 597 441, **1986**.
- Stapp, P. R. Report NIPER-434, Bartlesville, OK, December, **1989**.
- Weisman, J. G. and Kessler, R. V., *Appl. Catal.* **1996**, 140, 1.
- US Patent 5 105 877, **1992**.
- US Patent 4 505 808, **1985**.
- Roychaudhury, S., Rao, N. S., Sinha, S. K., Gupta, K. K., Sapkal, A. V., Jain, A. K., Saluja, J. S. SPE N° 37547, presented in Int. Thermal Oper. Heavy Oil Symp. Bakersfield, CA, Feb. 10-12, **1997**.
- Wichert, G. C., Okazawa, N. E., Moore, R. G., Belgrave, J. D. M. SPE N° 30299, presented in Inter. Heavy Oil Symp., Calgary, Alberta, Canada, June 19-21, **1995**, 529.
- Weissman, J. G., Kessler, R. V., Sawicki, R. A., Belgrave, J. D. M., Laureshen, C. J., Metha, S. A., Moore, R. G., Ursenbach, M. G. *Ener. & Fuel* **1996**, 10, 883.
- US Patent 5891829, **1999**.
- Vallejos C., Vasquez T. and Ovalles C. *Am. Chem. Soc., Div. Petrol Chem. Prepr.* **2000**, 45 (49), 591.
- Scott C., Alfonso H., Delgado O., Pérez-Zurita M. J., Bolívar C. and Ovalles C. *Am. Chem. Soc., Div. Petrol Chem Prepr.* **2000**, 45 (49), 588.
- US Patent 5 105 887, **1992**.
- Burger, J., Sourieau, P., Combarnous, M. 'Thermal Methods of Oil Recovery', Techni, Paris, **1985**, p. 81.
- Yu, J. and Savage, P. *Ind. Eng. Chem. Res.* **1998**, 37, 2
- Wang, B., Hou, H., Gu, Y. *J. Phys. Chem. A*, **2000**, 104, 10526.

THERMAL PROPERTIES AND DISSOLUTION BEHAVIOR OF ASPHALTENES

Yan Zhang^{*1}, Toshimasa Takanohashi¹, Sinya Sato¹, Ikuo Saito¹ and Ryuzo Tanaka²

¹Institute for Energy Utilization,
National Institute of Advanced Industrial
Science and Technology,
16-1 Onogawa, Tsukuba 305-8569, Japan

²Central Research Laboratories,
Idemitsu Kosan Co., Ltd.
Kamiizumi1280, Sodegaura, Chiba 299-0293, Japan

Introduction

Asphaltenes are very complex mixtures containing more than tens of thousands of compounds with different functionalities and a wide molecular weight distribution. To date, characterization for asphaltenes was almost focused on the chemical structural parameters, compositions, or aggregates sizes¹⁻². For some processes, however, in addition to such knowledge of the chemical structure and composition, information of thermal properties can be needed. The latter may be more helpful for understanding the thermodynamic behavior of asphaltenes in various reactions.

Asphaltene molecules are known to form aggregates through various noncovalent interactions in crude oils or vacuum residues (VR), which can be responsible for the formation of coke-precursor as well as the deactivation to catalytic reactions in upgrading and refining processes. Our recent results suggested that coke formation can be decreased by dissociation of asphaltene aggregates in organic solvents.³ In order to control the relaxation of the aggregated structure in solvents more effectively, it is important to acquire the knowledge about the thermal properties of asphaltenes, and the interactions between asphaltene and solvent molecules.

In the present study, the thermal properties of asphaltenes, and their heats of solution in organic solvents were measured using differential scanning calorimetry (DSC) and microcalorimetry, respectively. By combination of the two techniques, the contribution of the thermal properties to the heat of solution, and the interaction between asphaltene and solvent molecules were investigated.

Experimental

Samples. Asphaltenes (AS) fractionated from Iranian Light (IL) and Maya (MY) vacuum residues (VR, after 500 °C vacuum distillation of the crude oils). A resin fraction (Re) from Maya VR was also used for comparison. Both asphaltenes and resin are solid powders at room temperature.

Differential scanning calorimetry measurements. Thermal properties of the samples were measured with a Seiko DSC 120 calorimeter. Temperature and enthalpy were calibrated with high purity indium, tin, lead and zinc, and the heat capacity was calibrated with synthetic sapphire. In a typical run, 6-10 mg of sample was heated at a heating rate of 10 °C/min from 8 to 300 °C under 50 mL/min nitrogen flow. For a repeated scan, after the first scan the sample was quickly quenched to 8 °C and heated again in the same way.

Microcalorimetry measurements. Heats of solution of the samples were measured by using a micro-twin-calorimeter (MPC-11, Tokyo Riko Co., Ltd.). Quinoline was used as a solvent. The detailed procedures have been reported in a previous paper⁴.

Results and Discussion

It is known that the enthalpy change during mixing of a nonpolar liquid solute with a nonpolar solvent arises from interactions between the solute and solvent. If the mixing process is assumed to occur at a constant volume, the heat of mixing follows Van Laar-Hildebrand equation⁵:

$$\Delta H_{\text{mix}} = kT\chi_h n_1 \phi_2 \quad (1)$$

where n_1 is the mole of solvent; ϕ_2 is the volume fraction of solute; χ_h is the interaction parameter between the solute and solvent. However, when a solid-state solute dissolves in a solvent, there will be an exothermic effect due to the dissolution of the glass^{6,7}, and/or an endothermic effect due to the fusion of crystalline structure⁸. In this case, the heat of solution (ΔH^M) should be the sum of the heat of mixing and the enthalpy change due to the phase transition (ΔH_{tran}) :

$$\Delta H^M = \Delta H_{\text{tran}} + \Delta H_{\text{mix}} \quad (2)$$

where

$$\Delta H_{\text{tran}} = \lambda + \Delta C_p (T - T_m) \quad (3)$$

here λ is the heat of fusion; ΔC_p is the difference of heat capacity between solid and liquid states, and T_m is the melting temperature. The ΔH^M can be directly determined by the microcalorimeter, and ΔH_{tran} can be estimated by using DSC. Thus, the heat of mixing ΔH_{mix} can be estimated based on the values of ΔH^M and ΔH_{tran} , which reflects the essential interactions when mixing a liquid solute with a solvent.

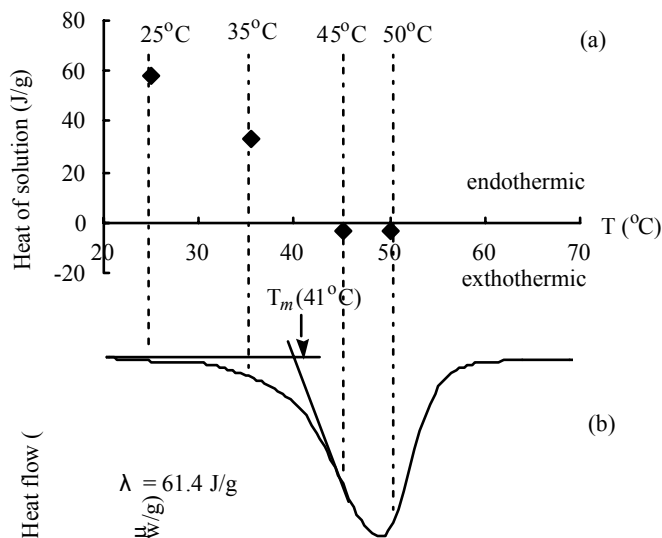


Figure 1. Heat of solution of *N,N*-dimethylnaphthylamine in quinoline (a) and its DSC thermogram (b).

As an example, Figure 1 shows the heat of solution of *N,N*-dimethylnaphthylamine (DMNA) in quinoline (Figure 1a) and its DSC thermogram (Figure 1b). According to DSC thermogram, the melting point and heat of fusion (λ) are determined as 41 °C and 61.4 J/g, respectively. Because no baseline shift was observed on the DSC diagram before and after melting ($\Delta C_p \approx 0$ J/g °C), the second term in equation (3) could be neglected. Thus, the enthalpy change (ΔH_{tran}) during the phase transition was approximately equal to the heat of fusion (λ). On the other hand, as shown in Figure 1a, in quinoline the

heat of solution below the melting temperature T_m was endothermic, while that above T_m was exothermic. At 25 °C, DMNA was completely solid, and the heat of solution was 58 J/g. Based on equation (2) and (3), the ΔH_{mix} can be calculated as -3.4 J/g (exothermic). This value was nearly the same to the measured ΔH_{mix} above T_m , -3.7 J/g at 45 °C and -2.9 J/g at 50 °C (Figure 1a). Thus, ΔH_{mix} can be directly measured above the melting point of solute by using the microcalorimetry. However, for other solutes having their melting temperatures beyond the limit of operating temperature of the microcalorimeter, the value of ΔH_{mix} can not be measured. Thus, by the combination of DSC and microcalorimetry, for various kinds of solutes ΔH_{mix} can be estimated.

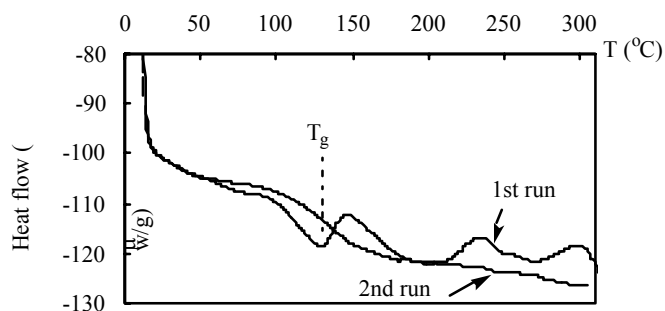


Figure 2. DSC thermogram of ASMY.

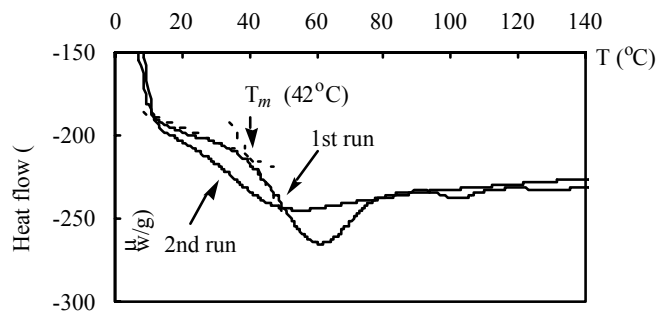


Figure 3. DSC thermogram of ReMY.

Figure 2 shows the DSC thermogram of ASMY. Three endothermic peaks were observed on the 1st scan. While on the 2nd scan, all the peaks disappeared and only baseline shift was observed in the temperature range from 100 to 180 °C. The similar behaviors were also observed for ASIL. The disappearance of three peaks on the 2nd scan indicates that all changes occurring during the first heating run were irreversible. On the other hand, the reversible baseline shift on the 2nd scan may provide evidence that asphaltenes have glass transition property.

Figure 3 shows the DSC thermogram of ReMY. Different from the thermal behavior of asphaltenes, the changes started from very low temperature near 42 °C (the 1st scan), and ReMY didn't seem to show such a glass transition in the temperature range studied as shown on the 2nd scan.

Table 1. Thermal Properties and Heats of Solution for Asphaltenes and Resin.

	ΔH^M	T_g	λ	ΔC_p	ΔH_{tran}	ΔH_{mix}
	J/g	°C	J/g	J/g°C	J/g	J/g
ASIL	-20.2 ^a	136	9.1	0.127	-14.1	-15.2
ASMY	-22.1 ^a	139	7.8	0.115	-13.3	-16.2
ReMY	6.1 ^a	-	4.6	0.129	-1.8	3.3 (4.4 ^b)

^aMeasured at 25°C in quinoline. ^bMeasured at 50°C in quinoline.

Table 1 summarizes the thermal properties of asphaltenes and resin determined by DSC, and their heats of solution in quinoline measured by microcalorimeter. It should be noted that heat of fusion (4.6 J/g) for ReMY determined by DSC, was close to the heat of solution in quinoline at 25 °C (6.1 J/g). By considering the difference of heat capacity ($\Delta C_p=0.129$ J/g °C) between solid and liquid ReMY, the calculated ΔH_{mix} (3.3 J/g) is nearly in accordance with the measured one (4.4 J/g at 50 °C). The endothermic nature of ΔH_{mix} for ReMY suggests that resin molecules are solvophobic to quinoline.

Table 1 also shows that for asphaltenes their glass transition energy (ΔH_{tran}) makes a large contribution to the heat of solution. According to other thermal properties determined by DSC and the heat of solution in quinoline at 25 °C, ΔH_{mix} were estimated as -15.2 and -16.2 J/g for ASIL and ASMY, respectively. These values reflect the enthalpy change due to the favorable interaction between asphaltenes and quinoline. Thus, the exothermic nature of ΔH_{mix} suggests that asphaltenes are strongly solvophilic to quinoline.

References

- (1) Su, Y.; Artok, L.; Murata, S.; Nomura, M. *Energy Fuels*, **1998**, *16*, 1265.
- (2) Sheu, E. Y.; Ling, K. S.; Sinha, S. K.; Overfield, R. E. *J. Colloid Interface Sci.* **1992**, *153*, 399.
- (3) Takanohashi, T.; Sato, S.; Tanaka, R. *Petr. Sic. Technol.*, in press.
- (4) Zhang, Y.; Takanohashi, T.; Sato, S.; Saito, I. Tanaka, R. *Energy Fuels*, **2003**, *18*, in press.
- (5) Hidebrand, J. H., Scott, R. L. *The solubility of Non-electrolytes*, Reinhold, New York, 1950, Chapter 20.
- (6) Bianchi, U.; Pedemonte, E.; Rossi, C. *Makromol. Chem.*, **1966**, *92*, 114.
- (7) Cottam, B. J.; Cowie, J. M. G.; Bywater, S. *Makromol. Chem.*, **1965**, *86*, 116.
- (8) Schreiber, H. P.; Waldman, M. H. *J. Polymer Sci.* **1967**, *A2*, *5*, 555.

New Methods for Characterization of Products from Micro-activity Testing (MAT) of Residue from Estonian Shale Oil

Yevgenia Briker, Zbigniew Ring, and Angelo Iacchelli

National Centre for Upgrading Technology, 1 Oil Patch Drive,
Devon, Alberta T9G 1A8, Canada

Abstract

The utilization of fossil fuels is going through drastic changes due to growing transportation fuel consumption and stricter environmental regulations. Both will result in an increase in the proportion of diesel fuel produced from synthetic crude oils, which in turn will lead to the expanding of existing and the development of new processing technologies. Most of the crude oils used for fuel production consist predominantly of hydrocarbons and contain only relatively small amounts of sulphur, oxygen, and nitrogen. Shale oils, in contrast, can contain large amounts of organic sulphur and /or oxygen compounds. Therefore, during processing of shale oils, in addition to making fuels, there may be an opportunity to extract valuable chemicals. Knowledge of the physical and chemical properties of these hydrocarbon materials is very important for the development of technologies necessary to fully utilize these materials.

In this paper we discuss the possibility of increasing the utilization of Estonian shale oil by application of the fluid catalytic cracking (FCC) process to the atmospheric residue fraction boiling between 320 and 750°C. FCC, being the most common conversion process in the oil refining industry, uses micro-activity testing (MAT) as its research tool to test various feedstocks and catalysts. The main emphasis in this paper is on the development of characterization methodology to analyze mono- and di-hydric phenols in MAT products that are inherently produced in very small amounts (<2mL) and have a wide boiling range.

Introduction

Over the past 50 years, fluid catalytic cracking (FCC) has been the most important heavy gas oil conversion process. FCC generates products ranging from gases and light olefins, through naphtha to light cycle oil, and heavy cycle oil. In this paper we discuss the possibility of applying the FCC process (through the micro activity test - MAT) to the atmospheric residue derived from an Estonian shale oil. This oil is the source of fuel oils and synthetic gas, but it could also be a source of a number of chemicals such as antiseptic oil for wood impregnation, electrode coke, rubber softeners, casting binders, etc. The shale oil phenols are used as feedstocks for epoxy and other resins, and as glueing compounds, rubber modifiers, synthetic tanning agents, etc. The most valuable phenols are in the 200-360°C boiling range. Therefore, there is an interest in exploring the behavior of heavy residue in the cracking environment, particularly in terms of the production of phenols in the useful boiling range.

A characterization procedure described by Černý et al. (1) was adopted as the basis of the new separation procedure developed here for quantification and identification of various fractions from the total liquid product from catalytic cracking of residue from an Estonian shale oil. The extrography procedure was replaced with open column chromatography, and the elution solvents were used in the order reported earlier (2). A different way of calculating the material balance was proposed for the full boiling-range material.

Experimental

The residual material derived from an Estonian shale oil was used as the feed for the macro-activity testing. Some properties of the feed and the total liquid product (TLP) are presented in Table 1. Simulated distillation curves are shown in Figure 1.

Table 1. Properties of feed and TLP from MAT testing of residue from Estonian shale oil

Feed		Product	
BP, °C	%OFF	BP, °C	%OFF
IBP (301.2°C)	0.5	IBP (84.5°C)	0.5
FBP (750.0°C)	99.5	FBP (587.5°C)	99.5
IBP-360°C	4.16	IBP-200°C	13.81
360-525°C	60.91	200-360°C	36.69
Density, g/mL	1.0660	Density, g/mL	1.0106

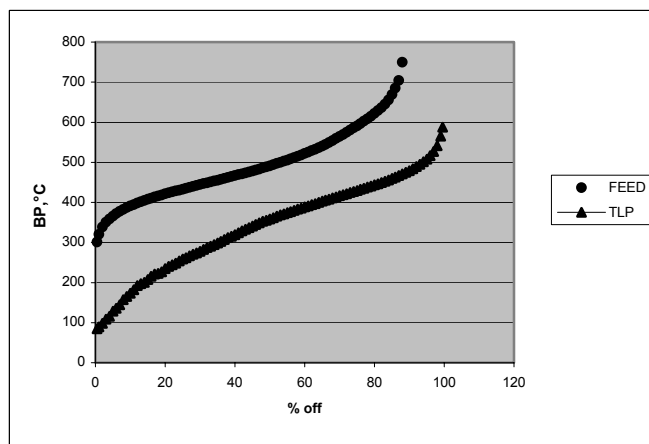


Figure 1. Simulated distillation of feed and TLP

The total liquid product (TLP) from the MAT was separated using the modified liquid chromatography method. This method was based on the extrography method described in the literature (1). The extrography column that was equipped with plunger pump and filled with basic alumina and silica in the original method was replaced with an open glass column (13.5-mm I.D. and a 450-mm length) filled with silica gel from Fisher Scientific (28-200 mesh) was activated for 12 h at 140°C. Its activity was adjusted by the addition of 4wt% water.

While in the original method, the analyzed sample was evenly distributed throughout the whole surface of the silica gel prior to extraction; in our modified method the total amount of TLP (0.7286 g) was applied on top of the column. The elution solvents were used in order of increasing polarity (2). Since TLP contained some of the material boiling below 200°C (13.81wt%), the calculation of material balance using gravimetric determination would not be suitable. Removal of solvents on vacuum rotary evaporator and vacuum dryer would result in the loss of light ends. In our case, the solution of each fraction was reduced to a known volume by using a mild rotary evaporation and a nitrogen gas sweep. The fractions were further analyzed by gas chromatograph-flame ionization detector (GC-FID). Quantification of fractions in the specified temperature intervals was performed by using the calibration standards prepared from previously separated fractions. All fractions were quantified only from 200°C, therefore the slight loss of the light ends encountered

during the nitrogen purge did not affect the results. The retention time calibration was performed by analyzing the normal paraffin standards at the identical conditions.

Results and Discussion

Micro activity testing of the material derived from an Estonian shale oil with IBP 301.2°C and FBP 750.0°C, yielded a product with IBP 84.5°C and FBP 587.5°C. From the simulated distillation data it was calculated that 13.81wt% of the material boiled below 200°C in the product. The yield of the material boiling between 200-360°C was 36.69wt%, while there was only 4.1wt% below 360°C in the feed. This temperature interval was important since it represented the fraction that might contain the phenolic compounds of interest, produced by cracking of heavy material.

The results of LC separation of TLP are presented in Table 2. The retention times for 200°C and 360°C were 5.727 min and 17.482 min respectively. The chromatograms of each fraction were integrated between these two points and the results were balanced with the results from the simulated distillation data.

According to the original method, the phenolic fractions are represented by fraction 4 (monohydric phenols) and fraction 5 (dihydric phenols). The GC-FID chromatograms of these fractions are shown in Figures 2 and 3.

Table 2. Results of LC separation of TLP from MAT testing of residue from Estonian shale oil

Fr. No	Solvent	Designation	200	200	IBP	360°C	IBP
			-	-	-	-	-
			360°C	360°C	200°C	FBP	FBP
			GC-FID	SimDist	SimDist	Sum	Sum
			Recovery, wt%	wt%	wt%	wt%	wt%
Fr.1	Hexane	Saturates	2.3				
Fr.2	Toluene	Aromatics	24.6				
Fr.3	Chloroform	Esters+	0.6				
Fr.4	Chlor./Dieth.Ether	Monophenols	5.2				
Fr.5	THF/Methanol	Diphenols	3.3				
Fr.6	Methanol	Polars	0.7				
Total			36.7	36.7	13.8	49.5	100.0

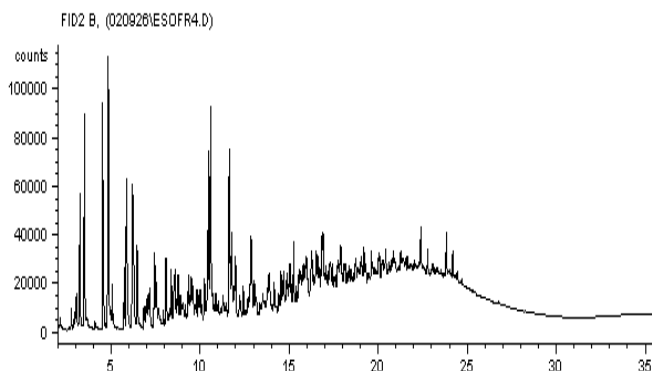


Figure 2. GC-FID chromatogram of Fraction 4

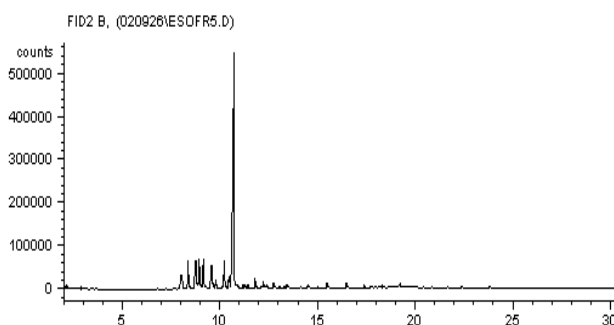


Figure 3. GC-FID chromatogram of Fraction 5

The combined phenolic fraction was the second largest (8.5wt%) after the aromatic fraction (24.6wt%). Both were analyzed by gas chromatography-mass spectrometry (GC-MS-equipped with mass selective detector from HP) with the library search option. Most of the peaks in Fraction 4 were designated as phenols with the largest peaks being cresols and 2,5-dimethyl phenol at 6.78 min, 6.86, min, 7.10, min, and 7.57, min. The rest of the chromatogram represents the variety of di- and tri-methyl phenols. There were no acids found in this fraction. Apparently, they decomposed during cracking. No clear assignments for peaks were given by the GC-MS in Fraction 5 due to a very low concentration of individual compounds. The largest outstanding peak was designated as phenol, 2,5-bis(1,1-dimethyl)-4-methyl.

Conclusions

Cracking of the residual material derived from an Estonian shale oil with a density 1.066 g/mL resulted in the production of a lighter liquid product with the density 1.0106 g/mL, and also resulted in quite a significant shift in the boiling point range. The starting material boiling between 301.2°C and 750°C was converted to a lighter material boiling between 84.5°C and 587.5°C.

The usefulness of this material in terms of the presence of phenolic compounds was verified by applying the separation technique, which was adapted from the original extrography method and modified into a simplified open column chromatography procedure. The new procedure was developed for analyzing the samples having a full boiling range.

The results of separation showed that useful phenols were produced as the result of catalytic cracking.

The project is ongoing and the full extend of catalytic cracking on the production of phenols and other streams at different conditions will be investigated, and the results will be published in future publications

Acknowledgment.

Partial funding for NCUT has been provided by the Canadian Program for Energy Research and Development (PERD), the Alberta Research Council (ARC) and the Alberta Energy Research Institute (AERI). This paper was partially funded by VKG of Estonia.

References

- (1) J. Černý, H. Pavlicová and V. Machovič, "Compound-class fractionation of coal-derived liquids by extrography", *FUEL*, 1990, Vol 69, 966-971.
- (2) M.M. Boduszynski, R.J. Hurtubise and H.F. Silver, *Anal. Chem.*, 1982, 54, 375.

Table 3. Peak assignments for Fraction 4 of TLP from MAT of Estonian shale oil

Peak RT,min	Assignment
5.70	phenol
6.78	phenol,2-methyl
6.86	phenol,2-methyl
7.10	phenol,3-methyl
7.57	phenol,2,5-dimethyl
8.03	phenol,2-ethyl
8.18	phenol,3,5-dimethyl
8.47	phenol,3-ethyl
8.60	phenol,2,3-dimethyl
8.84	phenol,2,4-dimethyl
8.99	phenol,2,3,6-trimethyl
9.32	phenol,2-ethyl-5-methyl
9.39	phenol,2-ethyl-6-methyl
9.47	phenol,3-(1-methylethyl)-
9.53	phenol,3-ethyl-5-methyl
9.77	phenol,2-(1-methylethyl)-
9.88	phenol,3,4,5-trimethyl
9.94	phenol,2,4,6-trimethyl
10.58	4-allylphenol
10.95	phenol, 3,5-diethyl
11.90	6-methyl-4-indanol
12.44	phenol, 4-(3-methyl-2-butenyl)-
13.06	1-naphthalenol
13.18	2-naphthalenol
14.33	1-naphthalenol,2-methyl
14.39	1-naphthalenol,3-methyl
14.64	1-naphthalenol,4-methyl
15.30	benzaldehyde, 2-chloro-6-fluoro-
15.48	1-naphthol, 5,7-dimethyl
16.37	2-hydroxy-1-naphthalenepropanol

Upgrading of Extra-Heavy Crude Using Hydrogen Donor under Steam Injection Conditions. Characterization by Pyrolysis GC-MS of the Asphaltenes and Effects of a Radical Initiator

Cesar Ovalles, Pablo Rengel-Unda, Jenny Bruzual and Arelys Salazar

PDVSA-Intevep
P.O. Box 76343, Caracas
Venezuela, 1070A
Email: ovallesc@pdvsa.com

Introduction

The development of a downhole upgrading process has always attracted the attention of the oil industry, mainly because of its advantages compared with aboveground counterparts. Lower lifting and transportation costs from the reservoir to the refining centers could be achieved. A volumetric well production increase can easily be achieved. A decrease in the consumption of costly light and medium petroleum oils used as diluents for heavy and extra-heavy crude oil production could be also obtained. Finally, higher value products (reduced viscosity and asphaltene, sulfur and heavy-metal content), with the concomitant reduction of refining severity would generate additional benefits.¹⁻⁵

However, technical challenges involve in the developing of an underground upgrading process are enormous. First at all, downhole processes are difficult to control and monitor under reservoir conditions. This is probably the main reason why these technologies are not widely used at the present time. Also, each well and reservoir requires individual treatment. This will increase the complexity of the field operations.⁵

Recently, a new concept was developed involving the underground addition of a hydrogen donor additive (tetralin), which in the presence of steam, natural formation (catalyst) and methane (natural gas) leads to extra-heavy crude oil upgrading.^{5,6} This process can be coupled to a steam stimulation process with 70-80% hydrogen donor recycling.^{5,6} In this work, the characterization of the asphaltenes by pyrolysis GC/MS is presented in order to gain insight into the mechanisms occurring during the extra heavy crude oil upgrading process. Also, the effect of a radical initiator on the properties of the upgraded products is also studied.

Experimental

The extra-heavy crude oil from the Orinoco Belt (Hamaca) used has the following properties: 9.1°API Gravity, 22.0% asphaltenes (heptane), 14.2% Carbon Conradson, viscosity (80°C) = 1810 ± 150 cP, 500°C⁺ residue = 71%, 7500 ppm nitrogen, 3.75% sulfur, 450 ppm of vanadium and 102 ppm of nickel. All percentages are reported by weight. A mixture of 1:1.7 tert-amyl-methyl ether (TAME) and methyl-tert-butyl ether (MTBE) was evaluated as radical initiator. The above mixture was used in a 1:1 ratio with hydrogen donor (tetralin).

Upgrading reactions were carried out in a stainless-steel 300-ml batch Parr reactor equipped with a heating mantle and a temperature controller. In a typical experiment, the reactor was loaded with sand (containing 10% of crude oil), water, and tetralin at a weight ratio of 10:1:1, respectively. The reactor was heated at 5°C/min to 315°C, generating a final pressure of approximately 1600 psi for 24 h (850 psi initial CH₄ pressure). After completing the experiment, water and tetralin were separated from the oil sand by vacuum distillation at 280°C. The residual tetralin was less than 0.05%, as revealed by H¹ NMR of the distilled fraction. The reactor was then cooled to room

temperature, and the remained oil was removed from the sand by solvent extraction with dichloromethane.

Crude oil mass balances were in the 93-99% w/w range. Percentages of recovery of tetralin were in the 92-105% range due to distillation of light fractions from the upgraded crude oils. Each experiment was repeated at least three times, the results presented herein correspond to an average of at least two different reactions with 90% confident using t-Student's value.

The asphaltene samples were isolated by precipitation with 50:1 v/v heptane:crude ratio followed by drying at 80°C for 1 h. The Py-GC/MS analyses were carried out in a RUSKA analyzer, model Thermachrom, coupled to a mass selective detector Hewlett-Packard, model HP5971B. Weighed samples were heated in a porous fused quartz crucible with continuous gas (helium) flowing through it. The asphaltene samples were heated from 70 to 600°C. Species evolved during the heating process were entrained in the flow and delivered to cryogenically cooled gas chromatograph (GC). Once sample heating is complete, the capillary column (DB-5, 30 m x 0.25 mm, 0.25 µm film thickness) is heated and trapped species were eluted into the mass analyser. The temperature program was 11 min at -35 °C, followed by a 10°C /min ramp rate to a final temperature of 300°C, the column was held at this temperature for 30 min. The mass spectrometer was operated at 70 eV in the electron impact mode. The mass range was from 50 to 650 amu. The pyrograms were analyzed by using the algorithms reported by Robinson⁷ and Piemonti.⁸

Results and Discussion

Table 1 shows the effect that radical initiator has on the extra-heavy crude oil upgrading process. A mixture of 1:1.7 TAME/MTBE was chosen because of its low cost (being refining stream) and the known ability to generate free radicals under low severity conditions.⁹ These additives were evaluated in conjunction with tetralin or by themselves.

Table 1. Effects of a Radical Initiator on the Upgrading of Extra-Heavy Crude Oil in the presence of tetralin under Steam Injection Conditions (315°C)^a

Additive (Reaction time)	°API (±0.5°)	% Asphalt. ^b (±0.3%)	Visc. ^c (cP) at 80°C
Hamaca Crude Oil	9.1	22.0	1810 ± 50
Tetralin-Control Exp. (0 h)	10.2	20.7 (6%)	1770 ± 160
Tetralin (24 h)	14.7	18.0 (18%)	110 ± 40
Tetralin + TAME/MTBE ^d (24 h)	15.0	18.2 (17%)	800 ± 140
TAME/MTBE ^e (24 h)	11.8	19.5 (11%)	1100 ± 300

^aExperiments were carried out under batchwise conditions, no stirring, at different reaction times. See experimental for details. Results are the average of at least two different reactions. ^bWeight percentages of asphaltenes. Numbers in brackets indicate conversions with respect to the original crude oil. ^cViscosity of the upgraded crude oil in cP measured at 80°C. Results presented with 90% confident using Student's value. ^dMixture of 1:1.7 tert-amyl-methyl ether (TAME) and methyl-tert-butyl ether (MTBE) was used in a 1:1 ratio with respect to tetralin. ^eSame radical initiator as before but no tetralin was used.

Firstly, control experiment (0 h) was carried in order to determine the effects of sample handling procedure (Table 1). The results showed an increase of only 1°API, 6% reduction of

asphaltenes, and slight decrease on viscosity (measured at 80°C). This is mainly due to the time needed to reach the distillation temperature (280°C). This time was approximately 30-45 min.

As observed in Table 1, the upgraded crude oil obtained from a mixture of hydrogen donor/TAME/MTBE has similar API gravities (ca. 15°) and asphaltene conversion (17-18%) and somehow a higher viscosity (800 vs 110 cP) than the one from the experiment with tetralin. In contrast, the upgraded crude oil generated by the use of the radical initiator alone present lower API gravity (12°API) and percentage of asphaltenes conversion (11%) with the concomitant higher viscosity (1100 cP) than the previous experiments. The latter experiment indicates that the presence of a hydrogen donor is necessary in order to maximize the properties of the upgraded crude oils, as reported in the literature.⁴⁻⁵

The best results were obtained when tetralin was used, as seen on Table 1. These indicate a general trend, i.e. effective crude oil upgrading can be achieved downhole at steam injection conditions, despite the intrinsic experimental error.

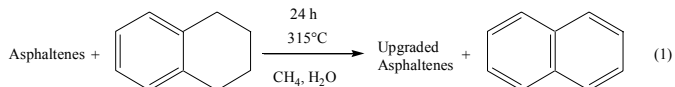
Table 2. Characterization by Pyrolysis GC-MS of the Asphaltenes Isolated from the Upgrading of Extra-Heavy Crude Using Hydrogen Donor under Steam Injection Conditions (315°C)^a

Types of Hydrocarbons ^b	Control Exp. ^c	Tetralin ^d	Tetralin + TAME/MTBE ^e	TAME / MTBE ^f
Total Saturates	46.9	47.2	48.9	47.8
Paraffins	9.0	9.8	10.6	9.9
Monocycloparaffins	9.1	9.7	10.3	9.8
Dicycloparaffins	8.1	9.1	9.3	9.4
Tricycloparaffins	20.6	18.6	18.6	18.7
Total Aromatics	53.1	52.8	51.1	52.2
Monoaromatics	21.5	20.8	20.6	21.3
Benzenes	6.8	6.7	7.0	6.8
Naphtenebenzenes	6.1	5.9	5.6	5.9
Dinaphtenebenzenes	8.6	8.2	8.0	8.6
Diaromatics	11.2	10.7	10.2	10.5
Naphtalenes	3.0	3.1	3.0	3.4
Acenaphtenes				
/Dibenzofuranes	3.0	2.7	2.4	2.5
Fluorenes	5.3	4.9	4.8	4.7
Triaromatics	2.6	3.2	3.0	3.3
Phenantrenes	1.0	1.4	1.5	1.5
Naphtenephenantrenes	1.6	1.8	1.5	1.8
Tetaromatics	4.2	4.4	4.2	4.2
Pyrene	2.9	2.9	2.9	2.9
Crysene	1.3	1.5	1.3	1.2
Pentaromatics	0.3	0.3	0.1	0.2
Aromatic tiophenes	12.0	12.0	11.6	11.5
Non identified	1.3	1.4	1.3	1.2

^aSame experimental conditions as Table 1. ^bWeight percentage as determined by INT101 algorithm. ^cControl experiment with 0 h at 315°C. ^dExp. were carried out using tetralin as hydrogen donor at 315°C for 24h. ^eExp. were carried out using a 1:1 tetralin:TAME/MTBE as hydrogen donors at 315°C for 24 h. ^fExp. were carried out using TAME/MTBE as hydrogen donors at 315°C for 24 h.

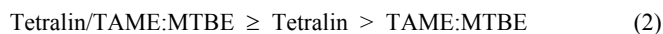
In order to get more detailed information about the composition of asphaltenes, the samples were further investigated by Py-GC/MS technique. In all cases, GC/MS analysis of pyrolysates yielded a complex trace containing an unresolved hump that was more or less pronounced depending on the asphaltene samples. Due to their complexities, the INT101 norm algorithm was applied.^{7,8} This norm is useful to check the quality of feeding streams and petroleum products. INT101 gives the hydrocarbon distribution in terms of weight and/or volume percentage of aliphatic and aromatic compounds. The results of this characterization are shown in Table 2. For the case of tetralin, the results show that the percentage of total saturates increase slightly and the aromatics decrease when compared with the control experiment. A more complete analysis of the

hydrocarbons detected in the control experiment and the one with tetralin indicates that the total aromatic fraction, mono- and di-aromatics decrease whereas mono- and dicycloparaffins increase. After hydrogen donor removal by vacuum distillation, naphthalene was detected in the distilled residue by gas chromatography. These results are consistent with a hydrogen transfer mechanism from the tetralin to the asphaltenes (eq. 1) at the low severity conditions (315°C).^{10,11}



In the case of the asphaltenes isolated from the crude oil treated with mixture tetralin/TAME:MTBE, there is an agreement with above results (Table 2). It was observed an increase in the total percentage of saturates with a decrease in the total percentage of aromatics in comparison with the control experiment. Also, lower percentages of mono- and diaromatics were found in the upgraded asphaltenes. These data are also similar to the experiment with tetralin. This result gives evidences to a hydrogen transfer mechanism (eq. 1) from the tetralin to the asphaltenes.^{10,11}

Using TAME/MTBE mixture alone, a slight reduction of the percentages of aromatic compound with the concomitant increase in the total saturates was observed (see Table 2). Therefore, the relative order of hydrogen transfer from donor to the extra heavy crude oil can be inferred as shown in eq. 2:



Conclusions

The characterization by pyrolysis GC-MS of the asphaltenes isolated from the upgraded crude oil under steam injection conditions gives evidence of a hydrogen transfer mechanism from the hydrogen donor (tetralin) to the hydrocarbon fractions.

The presence of a radical initiator (TAME:MTBE) has little effect on the properties of the upgraded crude oil steam injection conditions.

Acknowledgement. The authors would like to thank PDVSA-INTEVEP for permission to publish this manuscript.

References

- (1) Weisman, J. G., Kessler, R. V., *Appl. Catal.*, **1996**, *140*, 1 and references therein.
- (2) Weissman, J. G., Kessler, R. V., Sawicki, R. A., Belgrave, J. D. M., Lareshen, C. J., Metha, S. A., Moore, R. G., Ursenbach, M. G., *Energy & Fuels*, **1996**, *10*, 883 and references therein.
- (3) Vallejos, C.; Vasquez, T.; Ovalles, C. *Amer. Chem. Soc., Div. Petrol. Chem. Prep.*, **2000**, *45*, 591.
- (4) Ovalles, C., Vallejos, C., Vásquez, T., Martinis, J., Peréz-Peréz, A., Cotte, E., Castellanos, L., Rodríguez, H., SPE Paper No. 69692, Proc. SPE Inter. Thermal Oper. Heavy Oil Symp. held in Margarita, Venezuela, March 12-14th (2001).
- (5) Ovalles, C., Vallejos, C., Vasquez, T., Rojas, I., Ehrman, U., Benitez, J. L., Martinez, R., accepted for publication in *J. Pet. Sci. Tech.* **2003**
- (6) Vallejos, C.; Vasquez, T.; Ovalles, C., US Patent No. 5,891,829; **1999**.
- (7) Robinson, C., J., *Anal. Chem.*, **1971**, *43*, 1425.
- (8) Piemontí, C., *Amer. Chem. Soc., Div. Petrol. Chem. Prep.*, **1992**, *37*, 1521.
- (9) Urbano, N., Machin, I., Jamal, A., Golindano, T., Cotte, E., *Abstract Amer. Chem. Soc.*, **2002**, *224*, 277
- (10) Tagaya, H., Sugai, J., Onuki, M., Chibsa, K., *Energy & Fuels*, **1987**, *1*, 397.
- (11) Iino, M., Shen, J., *Energy & Fuels*, **1994**, *8*, 978.

ESTIMATION OF THE STRUCTURAL PARAMETER DISTRIBUTION OF ASPHALTENE USING PREPARATIVE GPC TECHNIQUE

Shinya Sato and Toshimasa Takanohashi

Institute for Energy Utilization
National Institute of Advanced Industrial
Science and Technology
16-1 Onogawa, Tsukuba,
Ibaraki, 305-8569, JAPAN

Ryuzo Tanaka

Central Research Laboratory
Idemitsu Kosan Co. Ltd.
1280 Kami-izumi, Sodegaura
Chiba, 299-0393, JAPAN

Introduction

In the investigation of the reactivity of heavy hydrocarbons, the structure of asphaltene is an important factor. Although asphaltene shows a wide variety of properties because it is a complex mixture of molecules with a wide range of molecular weights, most of the discussions have conventionally been based on the average molecular structure. Even though some researchers have been trying to reflect structural distributions into structural parameters, most of them are expressions of parameters such as molecular weight with an assumption of a mathematical distribution function¹⁾ and not an expression of distribution based on the results of analyses.

In a previous study, we found a tendency of the asphaltene properties to be that the aromaticity is high when the average molecular weight is low, whereas the aromaticity is low when the average molecular weight is high. Thus, in the present study, asphaltene was fractionated according to the molecular weight using Gel Permeation Chromatography (GPC), average structural analyses were carried out on each fraction, and the molecular weight dependency of the structural parameters was investigated.

Experimental

The asphaltenes used in this study were recovered from the vacuum residue distillation of Maya crude oil (AS-MY) from Mexico (Table 1). Two series of runs were carried out for AS-MY. In the first run, AS-MY was separated into 50 GPC fractions around the peak area through a Shodex KF-2003 GPC column using chloroform as solvent. This process was repeated 50 times and 500 mg of asphaltene was separated. Then the collected fractions were put together into 5 consolidated fractions so that the recovery rate of each fraction was about the same. Subsequently, average structure analyses³⁾ were carried out using the results from the GPC molecular weight measurement using Shodex K403F column,

Table 1 Properties of Asphaltene

Content in VR %	24.9
Elemental analysis, wt%	
C	82.0
H	7.5
N	1.3
S	7.1
Ni, ppm	390
V, ppm	1800
H/C	1.11
Carbon aromaticity	0.50
Molecular weight	
Number averaged	873
Weight averaged	2148
by LD/MS	1221

VR : Vacuum residue

elemental analysis, and ¹H- and ¹³C-NMR analysis²⁾ in order to investigate the molecular weight dependency of the representative parameters of the average structure.

In the second run, AS-MY was separated into 50 fractions by GPC. Then the 50 fractions were analysed as the same manner as those in the first experiment except ¹³C-NMR. The results were compared with those for the consolidated fractions.

Results and Discussion

GPC separation The recovery rate of asphaltene was calculated using the sum of the recovery amounts in the 30 fractions and the residual amount in the waste as 100 wt% value. The recovery rate from AS-MY in the 30 fractions was 69 wt%. For the second experiments, similar results were observed indicating a good reproducibility in the GPC separations.

Based on this value, the fractions were put together into 5 consolidated aliquot of the fractions so that each fraction consists of approximately 14 wt%. The physical properties of each fraction for AS-MY, summarized in Table 2, show that the properties were constant in fractions 1 to 3, but in fractions 4 and 5, the H/C values seem to be decreasing and the fa value increasing.

Table 2. Properties of fractionated asphaltenes for AS-M

Fraction	1	2	3	4	5
Recovery, wt%	18	13	13	16	10
Elemental analysis, wt%					
C	79.4	81.5	81.6	83.2	81.6
H	7.88	7.91	7.67	7.47	6.98
N	1.18	1.20	1.39	1.63	1.60
S	7.17	7.52	6.90	5.34	6.70
H/C	1.18	1.16	1.12	1.07	1.02
¹ H-NMR					
Ha	7.5	8.7	7.2	10.0	11.7
H _α	13.6	14.7	20.5	18.0	23.8
H _β	59.3	57.3	56.3	54.4	50.7
H _γ	19.7	19.3	15.9	17.6	13.8
fa	0.42	0.47	0.45	0.46	0.55
MW	6984	3318	1677	674	145

MW: number averaged molecular weight by GPC

Structural parameter distribution Average structural analysis utilizes a number of structural parameters for the consolidated 5 fractions. Among them, we have especially focused on H/C, N/C, S/C, terminal methyl group carbon (C_γ/C), fa (Ca/C), total ring numbers (Rt), and aromatic ring numbers (Ra) that are closely related to the structure of condensed rings which contain aromatic ring(s). However, there is no established consensus on the significance of molecular weight in GPC, so the average structural parameters obtained from the molecular weight in GPC were converted into values for a single carbon atom for this study. The parameters including H/C, N/C, S/C, and fa values were calculated directly from the analytical values. C_γ/C was calculated using H/C and the results of ¹H-NMR. Since Rt itself is dependent on the number of carbons, the Rt' value obtained by the equation 1 was used in the evaluation as the parameter of the total ring number.

$$Rt' = (Rt - 1)/C = 1 - (H/C + fa) / 2 \quad (1)$$

The structural parameters obtained in the above-mentioned way are summarized in Table 3.

Table 3. Structural parameters of fractions from AS-

Fractions	1	2	3	4	5
MW	6984	3318	1677	674	145
H/C	1.18	1.16	1.18	1.12	1.02
N/C	0.013	0.013	0.012	0.015	0.017
S/C	0.034	0.035	0.033	0.032	0.031
fa	0.45	0.46	0.46	0.48	0.58
Cr/C	0.077	0.074	0.058	0.062	0.046
Rt'/C	0.186	0.190	0.175	0.198	0.202
Ra/C	0.124	0.136	0.126	0.143	0.143

Among these parameters, H/C and fa varied through fractions 3 to 5, whereas other parameters did not vary as much. Indeed, Rt'/C values, which are a function of H/C+fa, showed as almost constant; the results suggest that the variations of H/C and fa were complementary.

When asphaltene is fractionated, H/C values can readily be obtained by elemental analysis, while the actual measurement of the fa value is relatively difficult due to the sample amount. Therefore, the relationship between them is thought to be very useful. Fig.1 shows that on the low molecular weight side with the boundary at around MW 1000 to 1500, the aromaticity decreases as molecular weight increases, whereas on the high molecular weight side, the parameters become constant.

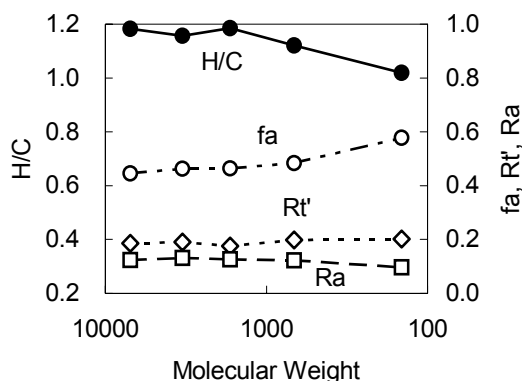


Fig. 1 Correlations of H/C and fa on MW determined by GPC

From the observed parameter variations, the following assumptions on the condensed rings of AS-MY were obtained: As molecular weight increases, (1) the lower the molecular weight is, the higher the aromaticity is; (2) up to MW 1000 to 1500, the molecular unit grows and the rate of having a side chain increases, therefore H/C increases and the fa value decreases; (3) over MW 1500, condensation or agglomeration of the fused ringsystem becomes predominant instead of the growth of the fused ring system.

For the fractions in the second experiments, the only the No.10-24 fractions can be analysed. The others were recovered too small amounts for the analyses. The trends for H/C and O/C, the content of O was the differential, are shown in Fig. 2. N/C and S/C are not varied. H/C curve had two boundaries. The higher boundary is around MW 1500, which is almost the same as MW in the first experiment. Fig. 2 also shows that low MW molecule contains more oxygen, indicating that small asphaltene molecule is significantly polar. The average molecular structure would be analysed from

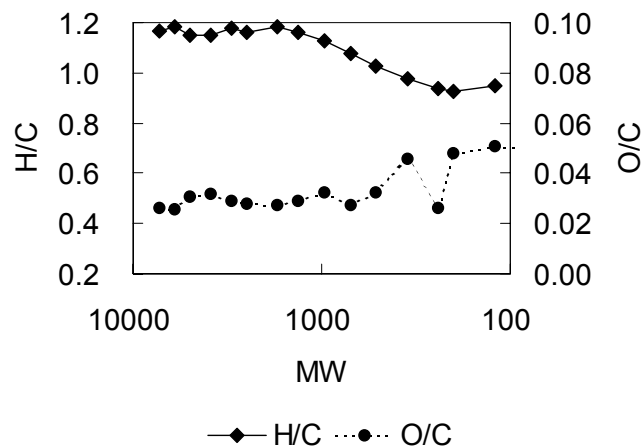


Fig. 2 H/C and O/C for 30 fractions separated by GPC

those data by estimating the fa using the correlation H/C + fa is constant.

Conclusion

AS-MY was separated into 5 and 30 fractions by two runs of preparative GPC, respectively. Average structural parameters were estimated by structure analyses for those fractions, and the trends of structural parameters per carbon were discussed.

H/C for both runs increased with increase in the molecular weight up to the molecular weight of 1000-1500, while fa was decreased with increase in the molecular weight in the same range. For the higher molecular weight, all parameters mentioned above, including H/C and fa, are almost constant. In the case of the first run, the sum of H/C and fa, which is related to the number of total rings, was almost constant in a wide range of molecular weight observed as well as the parameter for the number of aromatic rings. N/C and S/C were also constant for both runs.

It is thought that asphaltene molecule was monomer and the growth of core structure mainly occurred up to the molecular weight of 1000 - 1500, and the polymerisation or agglomeration of monomer was predominant for the higher molecular weight.

Acknowledgment

This study was supported by an International Joint Research Grant Program from New Energy and Industrial Technology Development Organization (NEDO) and carried out in collaboration between the National Institute of Advanced Industrial Science and Technology (AIST), the Central Research Laboratory, Idemitsu Kosan Co., Ltd., and the Argonne National Laboratory, USA.

References

1. Neurock M., Nigam A., Trauth D., Klein M. T., *Chem. Eng. Sci.*, **49**, 4153 (1994).
2. Sato S., Takanohashi T., Tanaka R., *Prepr. Am. Chem. Soc., Div. Fuel Chem.*, **46-2**, 353 (2001).
3. Sato S., *J. Jpn Petrol. Inst.*, **40**, 46 (1997).

Characterization of refractory sulfur compounds in residua: help for deep residue hydrodesulfurization

I. Guibard¹, F.X. Haulle¹, S. Kressmann¹, I. Merdrignac²

1-Institut Français du Pétrole, CEDI "René Navarre", BP3, 69390 Vernaison, France

2-Institut Français du Pétrole, 1-4 av de Bois Préau, 92852 Rueil Malmaison cedex, France

Introduction

The refinery of petroleum residues is more and more focussed on the removal of sulfur compounds from fuel oils. This low sulfur fuel oil (LSFO) is essentially used in power plant for electricity production that enables to reduce SO_x emissions. Moreover desulfurized fuel oil is necessary to have a suitable feed for Resid Catalytic Cracking (RCC) unit. Atmospheric residues (AR) and above all vacuum residues (VR) are the most difficult feeds to process catalytically as they contain and concentrate most of the crude impurities. Among them, asphaltenes, metals and heavy sulfur compounds affect the process performances.

These residues are generally hydrotreated in a fixed bed unit using high pressure of hydrogen and specific catalysts. The process consists of two complementary sections installed in series: the demetallization (HDM) section and the refining section (HDS). The main objective of the HDM section is to disaggregate asphaltenes and to remove most of the metals. However in this section a partial hydrodesulfurization (HDS) also occurs. In the HDS section the deeply transformed feed is refined to remove most of the sulfur content from the effluent and to reduce Conradson Carbon to product a RCC feed. Depending on case, an intermediate section could be included with a specific catalyst, which is able to continue the demetallization and to begin the desulfurization step (1,2). For each section, specific catalysts were developed in order to achieve high severity levels and high duration cycle lengths. The IFP Hyvahl residue upgrading process developed in 1982 (1) has a well adapted graded catalyst system that is able to cope with a wide range of feeds and to associate high severity levels together with constant product quality and increased cycle lengths. Since a few years, the demand for very low sulfur fuel oil (until 0.5 - 0.3 weight %) during long cycle has been increased on the worldwide market. This objective is difficult to achieve and requires increasing knowledge of heavy refractory sulfur compounds and kinetic information on the sulfur compound reactivity. But the characterization of sulfur compounds in fuel oil is complex due to the high boiling range of these products and the unavailability of detailed analytical technique as sulfur speciation for diesel.

The main purpose of this work is to characterize the refractory sulfur compounds in heavy oils using standard analyses in order to have a first approach of their location. In this study, the evolution of heavy sulfur compounds during hydrotreating process was followed along reactors.

Experimental

Feed and hydrotreatment experiments. A first set of experiments was performed on Middle East resid in order to locate sulfur compounds. Several feedstocks (AR, VR) were hydrotreated in a fixed bed reactor unit under the same standard operating conditions to achieve the target of 0.3%wt sulfur. Experiments were conducted using industrial residue hydrotreatment catalysts (HDM and HDS sections). The characteristics of these feedstocks are given in Table 1.

A second set of experiments was carried out only on HDM catalyst with varying residence time in order to study precisely the HDS performance.

Analytical techniques. Liquid products were distilled in three cuts (PI-375, 375-520°C and 520°C+). The heaviest cut is subjected for separation to asphaltenes (Asph) and maltenes fractions using n-heptane. The maltenes fraction and 375-520°C cut were further fractionated by liquid column chromatography into saturates (Sat), aromatics (Aro) and resins (Res). On each SARA fractions, elemental analysis (Carbon, Hydrogen, Nitrogen, Sulfur, Oxygen) was performed. Metal (Nickel and Vanadium) concentrations in asphaltenes and resins were measured by ICP method.

Size exclusion chromatography (SEC) was performed on the different fractions using a refractive index detector. Calibration was carried out using polystyrene standards (3).

Table 1. Main characteristics of Middle East feedstocks

	Arabian Medium AR	Arabian Light VR	Arabian Heavy VR
Total S (%wt)	3.7	4.5	5.3
Total Ni+V (ppm)	80	125	218
Asph (% wt)	6.3	9.9	16.2
S (%wt)	7.16	6.76	7.6
Res 520°C+	20	34.8	34.3
S (%wt)	5.66	5.4	6.4
Aro 520°C+	20	44.5	40.7
S(%wt)	3.82	4.0	4.5
Sat 520°C+	4.3	8.0	4.2
S(%wt)	0.1	0.9	-
520°C- cut	49.4	2.8	4.6
S(%wt)	2.6	3.5	3.9

Results and Discussion

Sulfur evolution during hydrotreatment. In atmospheric or vacuum residua, sulfur is initially concentrated in the heaviest fraction (cut 520°C+) and specifically in asphaltenes, which are described as the most refractory class to hydrodesulfurization (4). During hydrotreatment, the total sulfur content decreases all along reactors and can reach 0.3%wt at the outlet of the unit using appropriate operating conditions (temperature, residence time). In the same time, residue conversion occurs and heavy fraction as asphaltenes, resins and aromatics decrease to product lighter fractions. **Figure 1** shows the evolution of the sulfur content inside the SARAs fraction versus residence time for the HDM and HDS section, in the case of arabian medium AR hydrotreatment. All fractions are continuously desulfurized along reactors but at different rate. Thus for HDM section, we observe an important decrease of sulfur content for all the fractions. The HDM catalyst is able not only to disaggregate the asphaltenes but also to eliminate a great part of sulfur compounds.

In the HDS section, the desulfurization rate seems lower for each fraction but the removal of ultimate sulfur is much more difficult. The sulfur content in resins and aromatics fractions reach a low level due to the use of a specific catalyst whereas it still remains at a high level in asphaltenes. This indicates that the sulfur is located in high molecular weight and doesn't access to the active site in the porosity of the HDS catalyst. However, this specific porosity is necessary for efficient removal of sulfur in lower molecular weight fractions.

After HDM and HDS section, the residual sulfur (0.3%wt) is still concentrated in 520°C+ fraction. The sulfur distribution is about 15% in asphaltenes, 40% in resins and aromatics fraction, 5% in light

compounds (520°C-). Therefore the sulfur is concentrated in heavy aromatics and resins fractions. The sulfur compounds in the asphaltenes fraction cannot be eliminated even at high residence time in HDS section. Consequently the desulfurization of asphaltenes is essentially done in the HDM section. The same observation has been done for VR hydrotreatment.

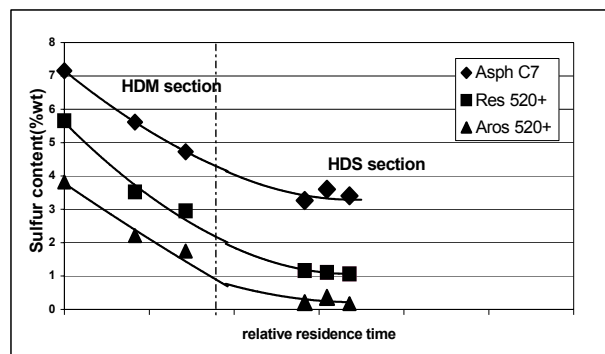


Figure 1. Arabian Medium AR hydrotreatment Sulfur content evolution in 520°C+ cut

In fact, it seems very important to study the evolution of sulfur compounds in the HDM section for different relative residence time. Experiments are carried out on Arabian heavy VR for the HDM section. We can observe an apparent slowing down of resin and aromatics desulfurization (see **figure 2**). The same experiments were conducted with desasphalted oil (DAO/C7) obtained from n-heptane precipitation of the same vacuum residue. The decrease of sulfur content in resins and aromatics fractions after DAO/C7 hydrotreatment is more important than for vacuum residue (see **Figure 2**). This shows the inhibitor effect of asphaltenes for HDS reaction. However aromatics and resins produced by hydrocracking of the asphaltenes may be also more refractory than the initial fractions that could explain the difference between DAO and VR (5).

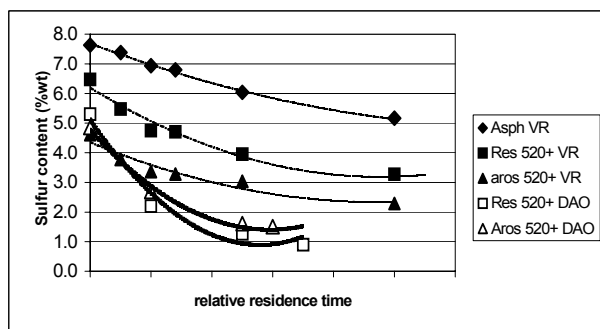


Figure 2. Arabian Heavy VR and DAO hydrotreatment in HDM section. Evolution of sulfur content in 520°C+ fractions

In conclusion, asphaltenes appear like the most difficult class to desulfurize and also have strong inhibitor effect on desulfurization reactions. Moreover, the presence of asphaltenes on the catalytic surface probably slows down the desulfurization rate of resins and aromatics fractions.

SEC analyses. In order to obtain more information about evolution of heavy compounds, Size Exclusion Chromatography (SEC) has been performed on asphaltenes fraction in Arabian medium AR before and after hydrotreatment. Profiles of relative distribution size are reported in **Figure 3**.

Results show that the structure of high molecular weight molecules is not affected in the HDM section, but an increase of the low to high molecular weight peaks ratio is observed. During this step smaller molecules can be formed. After the second step of the process (HDS), chromatogram profiles show however a significant decrease of the low molecular weight peak. Interpretations of such results may be a preferential conversion of small asphaltene molecules into resins and aromatics due the high level of hydrogenation of HDS catalyst. Besides, high molecular weight population seems to be equivalent after the first and the second step of the process. In conclusion, the highest molecular weight asphaltenes that are not eliminated on HDM catalyst are still remaining at the outlet process after HDS. This confirms the kinetic evolution of asphaltenes sulfur.

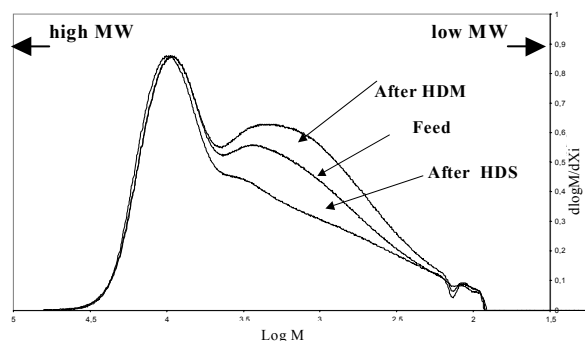


Figure 3. Arabian medium AR hydrotreatment SEC chromatograms of non converted and converted asphaltenes after HDM and HDS section of the Hyvahl process.

Conclusion

The increasing severity of sulfur specifications for fuel oil involves the need of more knowledge about the heaviest sulfur compounds. Deep desulfurization can be achieved with appropriate catalytic system and operating conditions. Usual analyses like liquid chromatography separation and elemental analysis give a first approach of the location of refractory compounds and can be a help to well-understand the specific role of each catalyst for HDS reactions. So, this study demonstrates that after deep hydrotreatment sulfur is essentially concentrated in heavy aromatics and resins fractions (cut 520°C+). The desulfurization of asphaltenes is difficult and occurs mainly in the HDM section. Moreover the presence of asphaltens on the catalytic surface slows down the desulfurization rate of others fractions.

The development of new appropriate analytical method seems to be required to isolate and characterize heavy sulfur compounds. This analysis should involve a better understanding of kinetic HDS reactions and should be a real help to define the best catalyst layout depending on the feed composition and origin.

References

- (1) Billon, A.; Peries, J.P.; Espeillac, M.; Des Courrières, T. NPRA 89th Annual Meeting, San Antonio, **1991**
- (2) Kressmann, S.; Harlé, V.; Kasztelan, S.; Guibard, I.; Tromeur, P.; Morel, F. Prepr. Pap - Am chem Soc., Div Fuel chem, **1999**
- (3) Merdrignac, I.; Truchy, C.; Robert, E.; Desmazieres, B.; Guibard, I.; Haulle, F.X.; Kressmann, S. Heavy Organics Deposition Conference (HOD), Puerta Vallarta, **2002**
- (4) Speight, J.G. In *The Desulfurization of heavy oils and residua 2nd edition*; Dekker, M., Inc : New York, 2000; pp. 127-167.
- (5) Haulle, F.X.; Kressmann, S. AICHE Spring Meeting, New Orleans, **2002**

CHARACTERIZATION OF SOLUBLE Mo COMPLEX DURING TRANSFORMATION TO Mo SULFIDE

Izumi Watanabe¹⁾, Kinya Sakanishi*²⁾, Isao Mochida¹⁾, and Masao Yoshimoto³⁾

- 1) Institute of Advanced Material Study, Kyushu University, Kasuga, Fukuoka 816-8580, Japan
- 2) National Institute of Advanced Industrial Science and Technology (AIST), Tsukuba West, Ibaraki 305-8569, Japan
- 3) Japan Cooperation Center, Petroleum(JCCP), 3-2-1 Sakado, Takatsu-ku, Kawasaki, Kanagawa 213-0012, Japan

Introduction

Highly dispersed Mo sulfide catalysts with fine particles have been reported very active for the hydrotreatment of heavy hydrocarbons such as vacuum residue (VR) and coal.¹⁻⁶ Several oil-soluble Mo complexes can be one of the most promising candidates for the application to slurry phase catalytic upgrading of vacuum residues, because they form very fine MoS₂ particles during their heating up to around 350 °C.⁷ It is reported that the difference in the catalytic activities of Mo-DTC (dithiocarbamate) and Mo-DTP (dithiophosphate) can be ascribed to the different extent of MoS₂ formation from the complexes under the hydrotreatment conditions. It is also noted that MoS₂ or solid Mo compounds derived from the two complexes are fine particles of very low crystallinity that can be highly dispersed in vacuum residue or asphaltene, because such solid particles are allowed to stay in asphaltene micelle which is dissolved or dispersed in toluene or maltene during the heating. Thermal decomposition of Mo-DTC stoichiometrically gave MoS₂, whereas Mo-DTP appears to provide MoS species in the presence of remaining phosphorous ligands. It seems that the remaining phosphorous ligands may retard the conversion of MoS to MoS₂ in VR, however, no clear evidence is not found by XRD, TGA, far-IR or TEM measurements.

In the present study, Raman spectroscopy is applied to the identification of MoS species formed from the soluble Mo complexes, since it can distinguish the layered graphite and amorphous-like carbon species. Because of the similarity in the layered structure of MoS₂ and graphite-like carbon, Raman spectroscopy is expected to give a clue to the difference in the structures of MoS species produced from the two Mo complexes.

Experimental

Materials. Mo-DTC and Mo-DTP used as MoS catalyst precursors in the present study are commercially available in the forms of crystal and solution, respectively. Their structures are illustrated in Fig.1. Commercially available MoS₂ powder is used as a reference compound. An Arabian heavy vacuum residue (AH-VR) is used for the hydrotreatment with Mo-complexes.

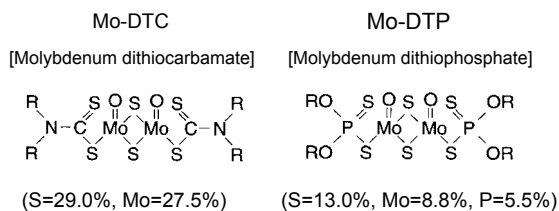


Fig.1 Structures of Mo-DTC and Mo-DTP

Heat-treatment. The mixture of Mo complex with VR was heated at 110 °C for 1 h for well dispersion, and then hydrotreated at 380 °C over the decomposition temperature of the complexes in a mini-autoclave under 10 MPa H₂. The heated mixture was extracted with n-hexane to separate the maltene and asphaltene fractions.

Analyses. The thermal behavior of the Mo complexes was examined using TGA (Seiko, SSC/5200) by their weight changes. The complexes and their decomposed products in the residue were analyzed by FT-Far IR (Jasco-620), XRD, and Raman spectroscopy.

Results and Discussion

According to TG/DTA profiles of Mo-DTC, three endothermic peaks were observed, and the first two of them were derived from the structural change in the ligands with a small weight change. The last peak around 300 °C was ascribed to the formation of MoS₂ with a large weight loss. This was in good agreement with the formation of Mo-S bond observed by far IR spectroscopy in Fig.2.

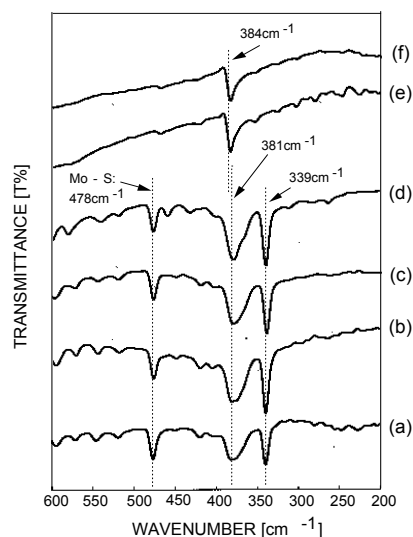


Fig.2 Far IR spectra of Mo-DTC before and after heat-treatment (a: non-treated, b: 200°C, c: 250°C, d: 260°C, e: 300°C, f: 400°C)

The decomposition of Mo-DTP was started from 200 °C based on the TG/DTA, reaching to 26 wt% at around 300°C, however, no clear peak of Mo-S was observed in the far IR as shown in Fig.3.

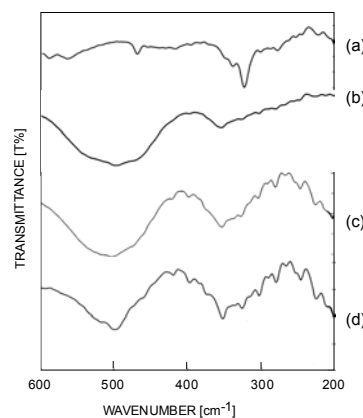


Fig.3 Far IR spectra of Mo-DTP before and after the heat-treatment (a: non-treated, b: 350°C, c: 400°C, d: 500°C)

When Mo-DTP was heat-treated under the atmosphere of 10% H₂S in H₂, the formation of Mo-S species was observed by Raman spectroscopy as shown in Fig.4.

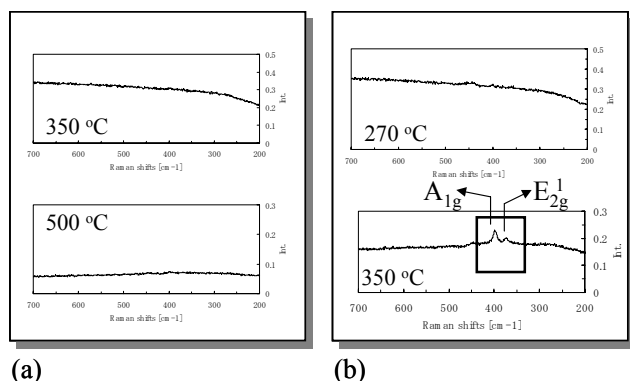


Fig.4 Raman spectra of Mo-DTP before and after the heat-treatment (a: under N₂, 1h; b: 10%H₂S/H₂, 1h)

It is revealed that MoS₂ should be produced from Mo-DTP over its decomposition temperature under the sufficient sulfiding conditions. It is pointed out that Mo-DTC produced MoS₂ at around 300°C even under the N₂ atmosphere as illustrated in Fig.5.

The difference in the properties and crystallinity of MoS₂ between Mo-DTC and Mo-DTP may reflect in the Raman spectroscopy. Further details on the transformation of MoS₂ morphology and crystallinity during the hydrotreatment are now on investigation

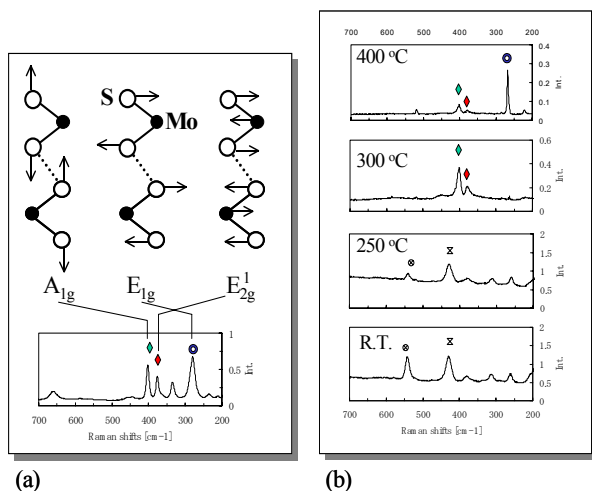


Fig.5 Raman spectra of Mo-DTC before and after the heat-treatment (a: MoS₂; b: heat-treated Mo-DTC under N₂)

Fig. 6 shows TEM micrograph of Mo-DTC heat-treated with asphaltene at 370°C. A clear formation of lamella-like MoS₂ crystalline structure was observed on the asphaltene matrix.

Fig.7 illustrates TOF-MAS spectra of asphaltene after the hydrotreatment with or without Mo-DTC or Mo-DTP. Compared to the spectra without catalyst, both of the Mo complexes hydrocracked the asphaltene fraction significantly, the cracking extent being a little higher with Mo-DTP. The yield of the asphaltene was lower with Mo-DTC than that with Mo-DTP, reflecting the higher hydrogenation activity of Mo-DTC.

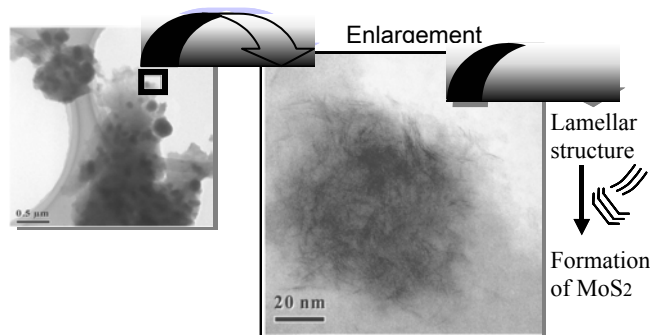


Fig.6 TEM of Mo-DTC treated at 370°C with asphaltene

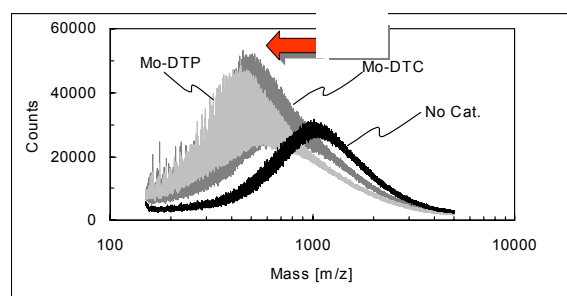


Fig.7 TOF-MAS of asphaltene after the hydrotreatment with or without Mo complex catalysts

References

1. Strausz, O.P., Lown, E.M., Mojelsky, T.W., *Prepr.ACS Div. Petrol. Chem.*, 1995, 40(2), 741.
2. Del Bianco, A., Panarti, N., Marchionna, M., *Prepr.ACS Div. Petrol. Chem.*, 1995, 40(2), 743.
3. Fixari, B., Peureux, S., Elmouchnino, J., Le Percec, P., *Energy Fuels*, 1994, 8, 588.
4. Del Bianco, A., Panariti, N., Di Carlo, S., Beltram, P.L., Carniti, P., *Energy Fuels*, 1994, 8, 593.
5. Panariti, N., Del Bianco, A., Del Piero, G., Marchionna, M., Carniti, P., *Appl.Catal. A: Gen.*, 2000, 204, 203.
6. Panariti, N., Del Bianco, A., Del Piero, G., Marchionna, M., Carniti, P., *Appl.Catal. A: Gen.*, 2000, 204, 215.
7. Watanabe, I., Otake, M., Yoshimoto, M., Sakanishi, K., Korai, Y., Mochida, I., *Fuel*, 2002, 81, 1515.

THE EFFECT OF ANTI FOULING ADDITIVES ON HEAT-INDUCED DEPOSITION

John F. Schabron and Joseph F. Rovani, Jr.
Western Research Institute
365 North 9th Street
Laramie, WY 82072

Introduction

Heat-Induced Deposition The problem of fouling due to deposition occurs when heavy oil materials are heated, blended, or pyrolyzed in visbreaking or vacuum distillation processes. This type of deposition can result from the formation of asphaltene flocs when a residuum is heated above a temperature at which the intermediate polarity material no longer protects the polar asphaltene cores^{1,2}, but below temperatures at which pyrolysis occurs (340 °C, 644 °F). This flocculation is not the same as asphaltene precipitation due to weak solvent addition. The temperature-induced asphaltene flocculation appears to be reversible when the material is cooled, as long as the material has not been heated to temperatures above which pyrolytic reactions occur. The polar asphaltene flocs can result in deposition and fouling problems in both upstream and downstream operations.

Residua are considered to be suspensions of polar asphaltene materials dispersed in a solvent phase.³ Pal and Rhodes developed a model for emulsions that has been applied to petroleum residua.³ The model features resins and solvent layers around an asphaltene core and solvated cores interacting with one another in an ordered system. Additional solvent is trapped between the asphaltene structures. Pal and Rhodes⁴ considered a solvation shell magnitude term K ($K=KS \cdot KF$), representing the amount of solvent adsorbed around a particle (KS) and the solvent trapped in a group of particles in the ordered system (KF). When a residuum is heated, the value for K decreases with increasing temperature, and less material is associated with the asphaltene structures, resulting in a flocculation of the polar asphaltenic-type core material.^{1,2,5}

Using an apparatus constructed to quantify relative heat-induced deposition tendencies for petroleum residua, deposition density measurements were made for five residua materials.⁵ The results suggested that the heat-induced deposition process is not significant at 100 °C (212 °F). It begins at 175 °C (347 °F), and is very evident at 250 °C (482 °F). At the latter temperature, the deposition density correlates with the free solvent volume, which is calculated from weight percent heptane asphaltenes and the Heithaus p_a parameter. The deposits were found to be enriched in porphyrins, and in nickel and vanadium. Activation energies of the reversible removal of the protective shell surrounding asphaltene cores were calculated from relative viscosity measurements at several temperatures. The energies were 470, 750, 940, 1,100, and 1,600 cal/mol for Vistar, CA Coastal, Boscan, MaxCL, and Redwater, B.C. residua, respectively.

Experimental

Additive Spiking Two commercially available anti-fouling additives designated A and B were added to a Lloydminster vacuum residuum at a level of 0.20 wt.% (2,000 ppm). Portions of 150g residua heated to 100 °C were poured into four round bottom flasks. A fifth round bottom flask for the control Lloydminster residuum with no additive was similarly prepared. A volume of 225 mL of cyclohexane was added to the residua in the round bottom flasks. The flasks containing the residua and solvent were attached to a rotary evaporator, which was used as a mixing device to spin the contents in

a warm water bath at 65°C for about 30 minutes until the residuum was completely dissolved. The round bottom flask was removed and the contents were charged with a precise weight of additive. The flask was placed back on the rotary evaporator, and the cyclohexane was removed.

Heat-Induced Deposition Heat-induced deposition studies were conducted for the control Lloydminster residuum, the 0.2% A sample, and the 0.2% B sample using an apparatus described previously.⁵ This apparatus consists of a pivoting aluminum chamber that is continuously purged with flowing argon (Figure 1). A 1.75" diameter pre-washed aluminum pan containing 5 g of sample was

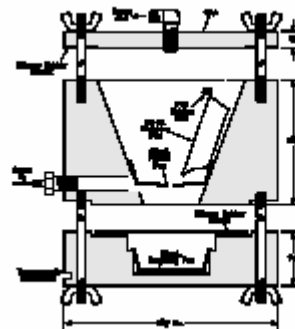


Figure 1. Heat-Induced Deposition Apparatus

placed inside the chamber in horizontal configuration. The chamber containing the sample was heated to 250 °C (482 °F) inside a convection oven, and at a predetermined timeframe, a trigger was released and the apparatus was rotated to position the sample pan in a vertical configuration (Figure 2). After a suitable timeframe to allow for the complete pouring of the sample from the sample pan into a collection pan, the oven was cooled, the chamber disassembled, and the sample pan examined for deposition phenomena. Deposition profiles were obtained at using a Kodak DC 265 zoom digital camera with a 37mm +10 macro lens.

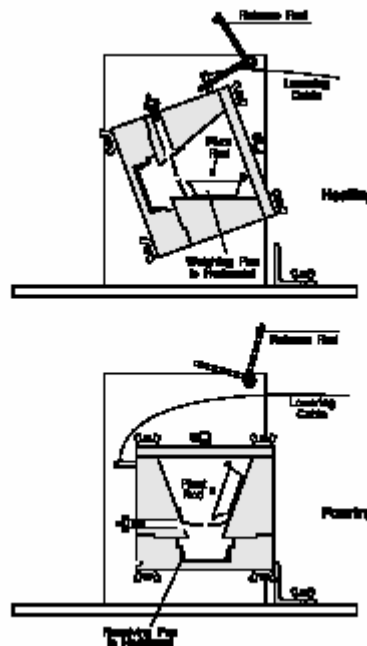


Figure 2. Use of the Deposition Apparatus

Results and Discussion

Deposition experiments were performed with three portions of whole Lloydminster residuum at 250 °C with no additives. Single runs were made with the residuum containing 0.2 wt.% of each of the two additives A and B. The deposition patterns showed the presence of agglomerated deposition spots from the residuum without additive. The materials with the additives showed some spots, but overall smoother deposition profiles were evident. This effect was difficult to visualize, but it appears to be real. Close-up images of the deposition patterns with and without additives are presented in Figure 3.



Figure 3. Heat-Induced Deposition Patterns

These show exaggerated detail of the deposition spots. The additives appear to suppress agglomeration and cause a smoother dispersion of the deposition pattern than when they are not present.

Conclusions

Non-pyrolytic heat-induced deposition experiments were performed at 250 °C with Lloydminster vacuum residuum with and without the presence of anti fouling additives. The results showed that both of the additives appear to cause a smoother, more well dispersed deposition pattern than was observed with the residuum without additives. The effect was somewhat difficult to visualize but it appears to be real. Thus, the additives could be causing an enhanced dispersion of the asphaltene cores which are exposed when the residuum is heated, depressing association and agglomeration of the polar cores.

Acknowledgments Funding for this study was provided by the U.S. Department of Energy cooperative agreement DE-FC26-98FT40322 and co-sponsors BetzDearborn, ChevronLummus, ConocoPhillips, and ExxonMobil. The authors would like to thank Tony Munari for preparing the figures.

Disclaimer This report was prepared as an account of work sponsored by an agency of the United States Government. Neither the United States Government nor any agency thereof, nor any of their employees, makes any warranty, express or implied, or assumes any legal liability or responsibility for the accuracy, completeness, or usefulness of any information, apparatus, product, or process disclosed, or represents that its use would not infringe privately owned rights. Reference herein to any specific commercial product, process, or service by trade name, trademark, manufacturer, or otherwise does not necessarily constitute or imply its endorsement, recommendation, or favoring by the United States Government or any agency thereof. The views and opinions of authors expressed herein do not necessarily state or reflect those of the United States Government or any agency thereof.

References

1. Storm, D.A., Barresi, R.J., Sheu, E.Y. *Energy and Fuels*, 1995, **9** 168–176.
2. Storm, D.A., Barresi, R.J., Sheu, E.Y. *Fuel Science and Technology International*, 1996, **14** (1&2) 243–260.
3. Pauli, A.T., Branthaver, J.F., *Preprints, Division of Petroleum Chemistry, American Chemical Society*, 1999, **44** (2) 190-193.
4. Pal, R., Rhodes, E., 1989, *Journal of Rheology*, 1989, **33** (7) 1021–1045.
5. Schabron, J.F., A.T. Pauli, A.T., Rovani, J.F., Jr., *Fuel*, 2001, **80** (7) 919–928.

CRACKING REACTIVITIES OF PETROLEUM ASPHALTENES

Ryuzo Tanaka^{*1}, Shinya Sato², Toshimasa Takanohashi², Satoru Sugita³

¹ Central Research Laboratories, Idemitsu Kosan Co., Ltd.
Sodegaura, 299-0293, JAPAN

² Institute for Energy Utilization
National Institute of Advanced Industrial Science and Technology
Tsukuba, 305-8569, JAPAN

³ Coal and Energy Project Department
Technical Development Group, Kobe Steel, Ltd.
Takasago, 676-8670, JAPAN

Introduction

Petroleum asphaltene is the heaviest portion of the oil fractions and may cause coking or plugging troubles in the refinery or in the transportation lines. Asphaltene is defined operationally by its solvent solubility, and it is an extremely complex organic mixture.

It is supposed that the cracking and coke formation reactivities of asphaltenes are dominated not only by their molecular structure but also by their aggregation tendency, because the size of asphaltene molecule is large and asphaltenes have various functional groups. The driving forces or the kinds of interaction contributing to the asphaltene aggregations have not yet completely clarified, because of the complexity of the phenomenon. Although, there must be some rigorously chemical relationships among the molecular structure, the aggregating tendency, and the coke making reactivity of asphaltenes.

Recently, some fundamental studies about molecular structure and aggregation phenomena of three petroleum asphaltenes, Maya, Khafji, and Iranian Light, with ¹³C-NMR¹), Molecular dynamics simulation²), SANS³), and SAXS⁴) were carried out. In this paper, coke-making reactivities of those asphaltenes on thermal cracking were investigated with some set of autoclave experiments. The main concern of the paper is whether the braking up of the asphaltene aggregates contribute to the coke suppression of the reactions.

Experimental

Sample Preparation. The residua (> 500 °C) was obtained by vacuum distillation of three crude oils. Asphaltenes were isolated by addition of a 20:1 excess of *n*-heptane to each of the residua at 25 °C. The suspension was stirred 1 h at 100 °C in the autoclave. After cooling down and leaving at 25 °C overnight, the suspension was filtered. The precipitate was washed with *n*-heptane twice and dried. The yields of asphaltenes (precipitates) of Maya, Khafji, and Iranian Light are 24.9, 14.2, and 6.3wt%, respectively. **Table 1** shows the elemental analysis data of the asphaltenes.

Table 1. Elemental analysis data of asphaltenes.

	Maya	Khafji	Iranian Light
elemental, wt %			
carbon	82.0	82.2	83.2
hydrogen	7.5	7.6	6.8
sulfur	7.1	7.6	5.9
nitrogen	1.3	0.9	1.4
oxygen	1.2	1.1	1.5
H/C	1.10	1.11	0.98
metals, wtppm			
Ni	390	200	390
V	1800	550	1200
density, g/cm ³	1.1767	1.1683	1.1669

Asphaltene of Maya (As-MY) is the heaviest and contains the most amount of metals among the three asphaltenes. As-KF is medium heavy and contains the least amount of metals. H/C atomic ratio of As-KF is the highest, and this could be interpreted as the lowest aromaticity. As-IL is the lightest, but contains much nitrogen and metals. It has the lowest H/C atomic ratio, meaning the highest aromaticity. These properties are considered to affect aggregation phenomena and coking reactivities of asphaltene molecules much.

Asphaltene cracking. All reaction experiments were carried out batch wise in a 30 mL micro reactor. In a typical experiment, 2g of asphaltene and 8 g of solvent were loaded into the reactor. A stainless ball was also loaded for stirring. The reactor was then pressurized with nitrogen of 5 MPa at room temperature and was immersed in a preheated tin bath at 300 °C. In the case with the relaxation of asphaltene aggregates, tin bath temperature was hold at the temperature for 60 min. Then the temperature of tin bath was rose with the heating rate of 2 °C/min until the temperature reached 440 °C, the nitrogen pressure becomes ca. 8 MPa at the temperature. The reactor was oscillated all the time in tin bath. After the reaction was completed, the reactor was cooled in air. In the case without the relaxation of asphaltene aggregates, the temperature of tin bath start rising just after the reactor was immersed in it. 1-methylnaphthalene (1MN), quinoline (Qui), decalin (Dec), and the mixture of Qui and Dec (50/50) were used as the solvent.

Separation. Gas yields were calculated from the weight decrease of the reactor with releasing gas pressure after reaction. Liquid product and coke were washed out of the reactor with tetrahydrofuran (THF), then THF was evaporated. The product were separated with *n*-heptane and toluene into three fractions, heptane-soluble (HS), heptane-insoluble and toluene-soluble (HI-TS), and toluene-insoluble (TI).

Results and Discussion

The yields of the asphaltene cracking without solvent are shown in **Figure 2** (NS: No Solvent, /R: with relaxation of aggregates). TI (Coke) yields are around 50% in these experiments. The order of the TI yields of three asphaltenes is MY > IL > KF. In the case of As-KF, the relaxation of asphaltene aggregates by stirring for one hour shows no effect for coke suppression.

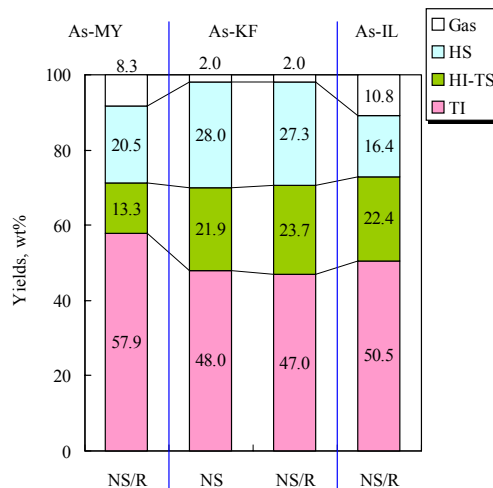


Figure 2. Yields of asphaltene cracking without solvent.

Figure 3 shows the yields of the asphaltene cracking with quinoline. The yields of TI from the asphaltene cracking decrease about 10 wt% and the order of TI yields from three asphaltene is the same with the case of without solvent (MY > IL > KF). With quinoline, the relaxation of asphaltene aggregates by stirring at 300 °C for one hour suppress the TI yields with ca. 5 wt% of all asphaltenes cracking.

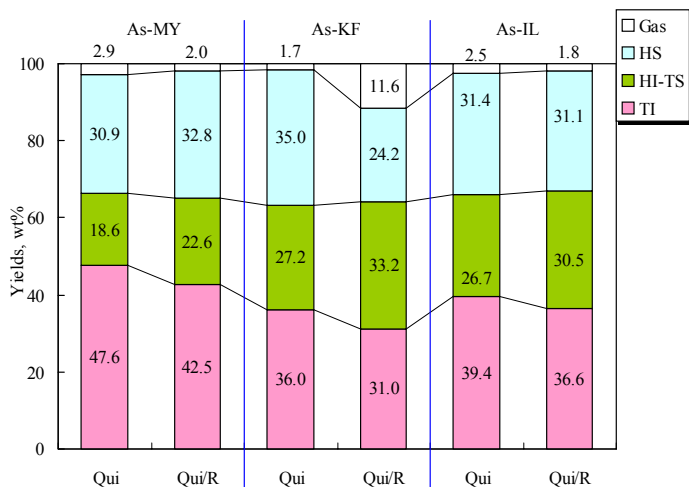


Figure 3. Yields of asphaltene cracking with quinoline.

Figure 4 shows the yields from As-KF. The order of TI yields with three solvents are 1MN > Qui > Q+D (quinoline and decalin mixture) >> Dec. Decalin shows the largest effect to suppress the coking and the TI yields of Q + D is almost average of Qui and Dec. In some literature, Dec is not a hydrogen donor at all. Although in this case, Dec seems to show the hydrogen donor ability. Indeed, the recovered solvent after reaction experiments contained the tetralin (tetralin content is 1.1 mol% of feed decalin).

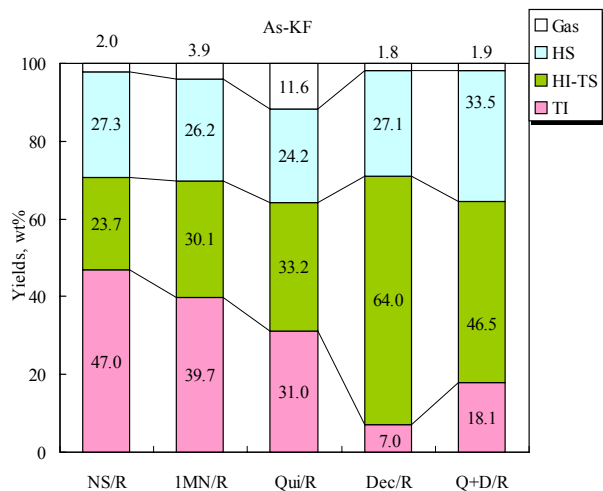


Figure 4. Yields of As-KF cracking without and with some solvents.

The yields of As-IL cracking have higher TI yields with each solvent than As-KF and show the same tendency depending on the solvent with As-KF. On the other hand, As-MY shows the different TI yields order with the solvents. The yields of As-MY cracking is shown in **Figure 5**. Different from As-KF or As-IL, As-MY is

converted into the least amount of TI with decalin and quinoline mixture solvent among four solvents.

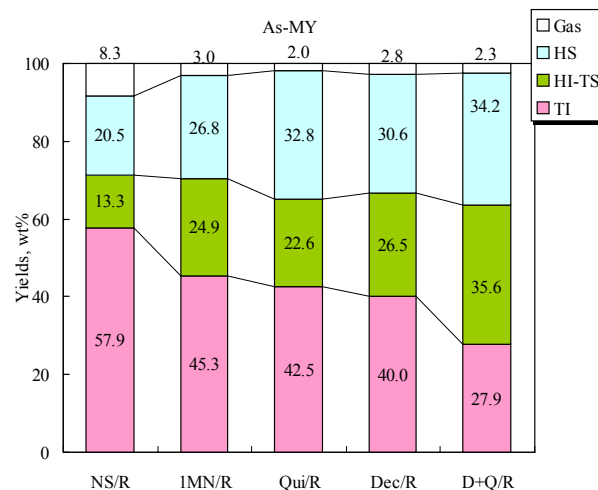


Figure 5. Yields of As-MY cracking without and with some solvents.

It may be interpreted that both aggregates of As-KF and As-IL brake up even in decalin at around reaction temperature and hydrogen is easily donated to the asphaltenes, but As-MY remains some aggregates in the decalin at around reaction temperature. In other word, quinoline assists the braking up of As-MY aggregates in the decalin and hydrogen donation to the asphaltene become easier. Results of SANS experiment indicate the large aggregates (fractal network) of Maya asphaltene exist in decalin solvent up to 350 °C. The feature of As-MY thermal cracking that higher coke yields than As-KF or As-IL and a multiplier effect to suppress the coke yields with Dec and Qui could be attributed to the fractal network.

Acknowledgment

This work was supported by the Proposal-Based International Joint Research Program, New Energy and Industrial Technology Development Organization (NEDO).

References

- Sato, S.; Takanohashi, T.; Tanaka, R. *Prepr. Pap. Am. Chem. Soc. Div. Fuel Chem.* **2001**, *46* (2), 353.
- Takanohashi, T.; Sato, S.; Tanaka, R. *Prepr. Pap. Am. Chem. Soc. Div. Fuel Chem.* **2001**, *46* (2), 357.
- Tanaka, R.; Winans, R.E.; Hunt, J.E.; Thiyagarajan, P.; Sato, S.; Takanohashi, T. *Prepr. Pap. Am. Chem. Soc. Div. Fuel Chem.* **2001**, *46* (2), 359.
- Tanaka, R.; Seifert, S.; Winans, R.E.; Hunt, J.E.; Thiyagarajan, P.; Sato, S.; Takanohashi, T. *Proceedings of 3rd International Conference on Petroleum Phase Behavior & Fouling*; AIChE, 2002; pp 20-23.

A PROCEDURE FOR ASPHALTENE ISOLATION AIMING CORRELATION WITH CARBON RESIDUE

Marco Antonio G. Teixeira

Petrobras R&D Center/Chemistry

Av. Um, Q. 7, Cidade Universitaria, 21949-900, Rio de Janeiro, Brazil, Fax: 55-21-3865-6296, marcoa@cenpes.petrobras.com.br

Abstract

The use of atmospheric residua as feedstocks for FCC units allows profitable conversion of heavy fractions. PETROBRAS has developed its own RFCC technology after a complete study of properties of the possible feedstocks for the 2 industrial units that are now operating in Brazil. A very important point in this characterization is the Ramsbottom carbon residue (RCR). Asphaltenes are well-known to be the main carbon residue precursors. However, no correlation could be found with the regular IP-143 asphaltene content. This paper describes considerations on the precipitation procedure and the necessity to eliminate aliphatic long-chained hydrocarbons (paraffin waxes) that co-precipitate with asphaltenes. This elimination had to be done by supercritical extraction, the only way found to achieve selectivity. The work yielded a linear correlation between asphaltene contents and RCR.

Introduction

It has been mentioned in literature^[1] that, though heavy petroleum fractions were limited to less economically attractive destinations, the increase in information about their constituents had been propitiating novel uses. About one of the most attractive ones, the conversion to light fuels, it has been recognized^[2] that the key to improvement of conversion is the development of better understanding of coke formation (normally referred to by carbon residue) chemistry mainly through the main precursors, asphaltenes. Carbon residue is one of the most important variables to be controlled in catalytical cracking and hydroprocessing^[3], and it limits the feedstock to be processed. Good predictions of carbon residua from asphaltene contents are not reached, however. This paper shows some reasons for that by the evaluation of asphaltene precipitation experiments and their products, and proposes a novel and efficient correlation.

Challenges in Correlation of Asphaltene Contents and Carbon Residue Values

There are clear descriptions in literature about asphaltenes of the chemical structure expected for these heavy petroleum fractions: large-sized aromatic nuclei, with aliphatic and naphthenic branches^[4]. However, it is not possible to reach an analytical method for selective separation of such materials. So, operational definitions are employed in this case. The most accepted one is the fact that asphaltenes are n-heptane insoluble, toluene soluble constituents of petroleum, which is the basis of the well-known IP-143 method^[5]. This definition has proved to be useful in many situations; literature cites for instance that a vacuum residue freed of n-heptane insoluble components does not show sludge in hydroprocessing, while the same residue does when it is integrally processed^[6].

Nevertheless, this criterium has shown to fail in being useful by itself in several situations. Sometimes this is not related to the precipitation approach employed, but to the very complex chemistry involved in conversion^[2]. But in the development of PETROBRAS's technologies for catalytical cracking of atmospheric residua (ARs)^[7], some of the inconsistencies of the criterium were made clear, and those were basically related to prediction of carbon residua. So,

efforts were developed to understand the reasons for that. Since asphaltenes are coke precursors, asphaltene contents should be strongly correlated to amounts of carbon residue. However, the first results of correlation obtained by the author, seen in figure 1, show that less than 50% of carbon residue formation is explained by the amounts of asphaltenes.

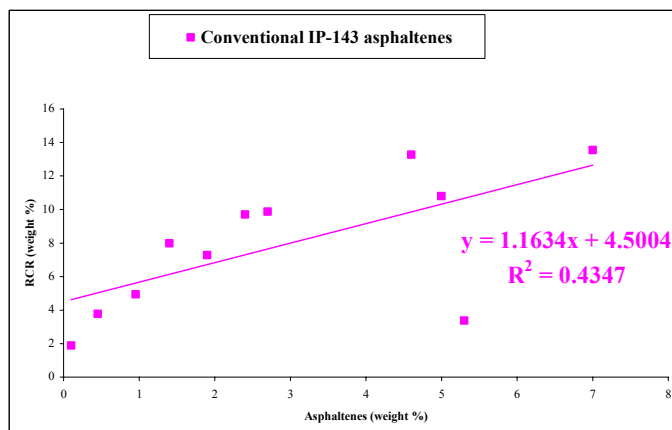


Figure 1. Plot of initial set of data for Ramsbottom carbon residue and conventional IP-143 asphaltene contents for various ARs, with very poor correlation

The reason to seek this understanding was not only the exact quantitative determination of carbon residue values from given characterizations of feedstocks, since Ramsbottom carbon residue values can be easily measured in refinery labs. The most important aim considered was the possibility to make clear this aspect related to the chemistry of carbon residue generation and its precursors, in such a way that information brought by this study could be useful for description of the phenomena involved and allow novel developments in conversion chemistry.

Asphaltene Precipitation

Investigation of asphaltene precipitation was the first step. Literature recommendations were developed for petroleum^[5], and that is an initial medium for asphaltene precipitation very distinct from ARs. The basis is that asphaltenes are not supposed to be dissolved in petroleum or its fractions; it has been assumed for a long time^[8,9] that they constitute micelles of aromatic materials maintained in suspension by other components, generically called resins, with similar characteristics but smaller molecular weights. Precipitation of asphaltenes depends on the ability of the precipitant to remove these resins around the asphaltenes and on the conditions it has to. That is why, in the comparison of 8 standardized methods for asphaltene precipitation from petroleum, different amounts of asphaltenes and *kinds of materials* can be found depending on the extraction procedure^[10], since the precipitation efficiency is not a process dictated by equilibrium. In the case of ARs, the action of the precipitant, due to the differences in diffusivities and viscosities, very important parameters for the precipitation mechanism described, is much more difficult than it is in precipitation from petroleum.

So, a novel procedure was proposed with increased contact times of precipitant with the ARs. Due to the possibility of oxidation in the long precipitation periods studied, experiments were not performed under reflux; room temperature was preferred. The ratio of precipitant (n-heptane) to oil was 40:1, according to limiting values from the literature^[11]. Table 1 shows selected results.

Table 1. Results for asphaltene contents of a AR from a mixture of the petroleum productions of Brazilian fields with varied contact time with precipitant

Precipitation time (h)	Asphaltenes precipitated (weight %)
2	4.20
60	5.57
240	5.81

Contact times of sixty hours were chosen, because after that the amount of further precipitated material is negligible. It can be seen that 2 hours, as recommended by IP-143 (though conditions mentioned there employ reflux), are not enough for precipitation of all of the asphaltene content by this novel approach. The correlation with carbon residue values was sought again. Figure 2 shows that correlation for the same set of data in figure 1. It can be seen that better explanation of RCR is obtained, and that supports very much the hypothesis of being asphaltenes important coke precursors.

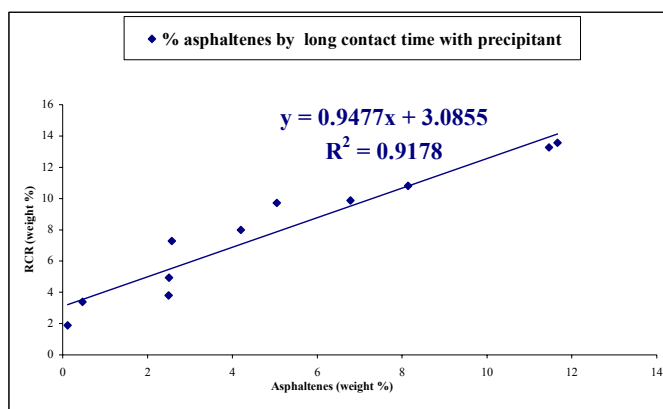


Figure 2. Plot of initial set of data of various ARs for RCR and asphaltene contents by the proposed method, considering only long contact time with precipitant, with very good correlation

The long contact time with precipitant could bring to the asphaltenes precipitated the possibility to explain more than 90% of the variations of carbon residue formation. The correlation indicates that about 3.1% of carbon residue would be expected if no asphaltene were present. The correlation is poor at low RCR values, but those are not the most worrisome cases. So, these first results were considered very promising ones.

The conditions of this precipitation method are not to be employed in refinery labs, of course, because precipitation times are prohibitive for operational needs. However, a databank could be made with this methodology for the most representative oils processed at PETROBRAS, since the approach showed to be useful. That was the next step in this research; about 20 ARs were chosen to compose that databank.

However, when twice as many ARs as we had in the initial set of data were analyzed, a new correlation showed that something had been missed when only the first set was considered, since the correlation was not as good as it was. That can be seen in figure 3. So, another aspect to explain these results was sought. Due to previous experiences with co-precipitation of asphaltenes and paraffin waxes in production facilities^[12], the possibility of interference by co-precipitation was studied.

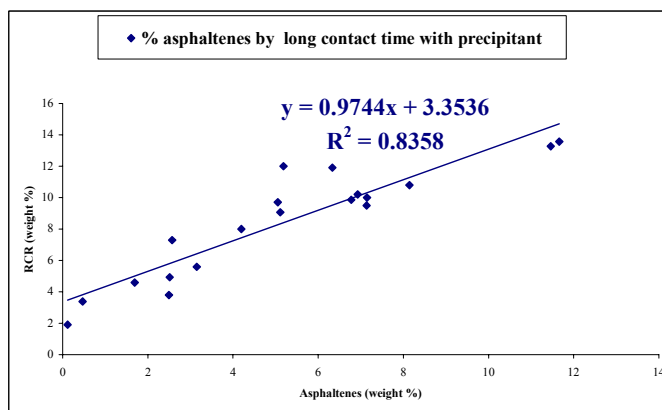


Figure 3. Plot of complete set of data of various ARs for RCR and asphaltene contents by the proposed method, considering only long contact time with precipitant

Correlation with Asphaltenes Precipitated by the Proposed Method after Extraction of Paraffinic Material

The possibility of co-precipitation had been considered since the first precipitation experiments, because the washing under reflux (that does not happen in this case, because of the preference for manipulation at room temperature) proposed by the conventional method should have as a major role the elimination of co-precipitated material. However, since good correlations were achieved, this problem was firstly assumed to be a minor one, if it existed. With the results in figure, they had to be considered.

The first approach was the comparison by the use of differential scanning calorimetry (DSC) measurements as it had been done in a previous work^[12]. Paraffinic materials show melting transitions upon heating. If they are co-precipitated with asphaltenes, DSC analysis data can identify their presence. That was detected in several samples.

Quantitative results from these data are possible if an average heat of fusion is known. If the values were consistent, the subtraction of the total amount of paraffins from the asphaltene contents measured by the proposed procedure should improve the correlation. That was tried with a value from literature^[13], but the correlation was even worst. Measurements for conventionally precipitated asphaltenes showed results in a similar order of magnitude as the ones found for the asphaltenes precipitated by the proposed method, indicating that co-precipitation does not happen only in the procedure discussed in the present work. This fact also indicates that even hot n-heptane is unable to dissolve these very long-chained aliphatic hydrocarbons.

For really quantitative results, a recently developed procedure^[14] for selective extraction of paraffins by supercritical fluid extraction with pure CO₂ was employed. This technique allows selective extractions and improved solvation capacity. The selectivity is necessary since asphaltenes are constituted by thousands, maybe millions of components, and some of them could be inadequately extracted if selective extractions were not achieved. Solvation capacity is necessary because heavy paraffins have insolubility as their most remarkable characteristic, as it is well known from oil transportation pipeline plugging problems, for example.

Asphaltenes precipitated by the method proposed here were extracted. Absence of paraffins in the final material was checked by DSC. The selectivity of the extraction was proved by analysis of the extracts by a recently proposed thermogravimetric approach^[15], in

which the distinct thermal behaviors of asphaltenes and paraffinic materials in coke generation are employed for characterization. Since the extracts can be weighed, gravimetric evaluation of paraffin-free asphaltenes was possible. Figure 4 shows the correlation obtained with this procedure. More than 90% of the variation in RCR is now explained by the amounts of asphaltenes. The slope is practically the unit, as expected. The linear coefficient shows that in the absence of asphaltenes, about 3.7% of carbon residue would be formed.

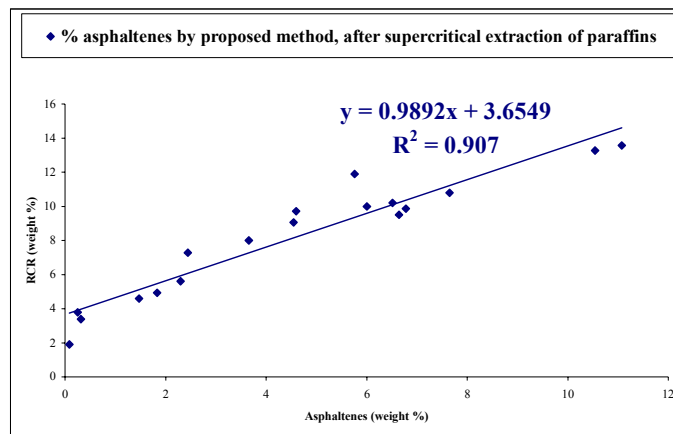


Figure 4. Plot of complete set of data of various ARs for RCR and asphaltene contents by the proposed method, considering long contact time with precipitant and supercritical extraction of paraffinic materials, with very good correlation

Conclusions

The work showed that asphaltenes yield amounts of coke equivalent to their contents in petroleum fractions. Those amounts can be predicted if paraffin-free asphaltenes are analysed after complete precipitation of asphaltenes. The precipitation is more difficult from heavy fractions, and long contact time with the precipitant should be employed. Selective and quantitative extraction of heavy paraffins can be achieved with supercritical extraction with pure CO₂. However, RCR values are not completely explained by asphaltenes by themselves; other components also yield carbon residua. Though these coke precursors were not identified in this work, the conclusion by the analysis of a universe of 20 atmospheric residua of several different origins is that a fixed contribution of 3.7% can account for that.

References

- (1) Yen, T. F. & Chilingarian, G. V., *18th AIChE et al Intersoc. Energy Convers. Eng. Conf. Proceedings 2*, pp.523-6 (1983)
- (2) Speight, J. G. *Kentucky University & U. S. DOE EAST. Oil Shale Symposium Proceedings*, pp. 17-27 (1992)
- (3) Sanford, E. C. *Energy & fuels*, 9(3), 549(1995)
- (4) Bestougeff, M. A. & Byramjee, R. J. "Chemical Constitution of Asphaltenes" in Yen, T. F. & Chilingarian, G.V. (Editors), *Asphaltenes and Asphalts, I. Developments in Petroleum Science*, 40, pp. 67-93
- (5) IP Standards Methods for Petroleum and its Products, The Institute of Petroleum, London (1965), Part I, Section 2, p. 596
- (6) Storm, D. A. et al., *Energy and Fuels*, 8, pp. 561-6 (1994)
- (7) Baptista, C. M. A.; Bonfadini, P. R. G.; Gilbert, W. R.; Teixeira, M. A. G. In. 2000 NPRA Annual Meeting, 2000, San Antonio Proceedings of the 2000 NPRA Annual Meeting, Washington D. C., EUA National Petrochemical & Refiners Association, 2000, #AM - 00-23

- (8) Mack, C. (1932), *Journal of Physical Chemistry*, 44, p. 2902
- (9) Sachanen, A. N. (1945)"The Chemical Constituents of Petroleum", Chapter 9, Reinhold Publishing Corporation, N. York
- (10) Speight, J. G. et al., *Fuel*, 63, pp.616-20 (1984)
- (11) Speight, J. G. & Long, R. B. "The Concept of Asphaltenes Revisited", *AIChE Spring National Meeting Preprint 78a*, 7 pp. (1995)
- (12) Teixeira, M. A. G.; Gonçalves, M. L. A. *Petroleum Science and Technology*, v. 18, n. 3-4, p. 273 -286, 2000
- (13) Burlé, B. et al., "Relationships Between Characterization of Asphalt Cements by Differential Scanning Calorimetry and Their Physical Properties", *Symposium on chemistry and Characterization of Asphalts Proceedings*, 330-7 (1990)
- (14) Teixeira, M. A. G.; Gonçalves, M. L. A. In. *219TH American Chemical Society Meeting, 2000, San Francisco, American Chemical Society, Division of Petroleum Chemistry Preprints*, p. #34
- (15) Teixeira, M. A. G.; Gonçalves, M. L. A. *Petroleum Science and Technology*, v. 17, n. 1&2, p. 1 -13, 1999

DETERMINATION OF COKING ONSET OF PETROLEUM FEEDSTOCKS USING SOLUBILITY PARAMETERS

Parviz M. Rahimi¹, Alem Teclerian¹, Ed Taylor¹, Theo deBruijn¹
and Irwin A Wiehe²

¹National Centre for Upgrading Technology (NCUT), 1 Oil Patch Drive, Suite A202, Devon, Alberta T9G 1A8 Canada

²Soluble Solutions, 3 Louise Lane, Gladstone, NJ 07934 USA

Abstract

Petroleum feedstocks are stable in nature, but if the fine balance in their chemical composition changes because of physical or thermal treatment, there is a possibility of solid formation due to asphaltene precipitation. Formation of asphaltene and high molecular weight components usually lead to coke and this has severe implications for refinery processing. For instance, significant coke formation can occur in heat exchangers, furnaces and fractionators during petroleum processing. It is important, then, to be able to predict the coking onset of different process streams and advise the operators to avoid process conditions (temperatures and space velocity) resulting in coke formation.

In the present work the coking onset of Athabasca bitumen was determined using a batch autoclave. Using the solubility parameters of the total liquid products, the onset of coke formation was determined. It was shown that coke formation was negligible up to a pitch conversion (conversion of resid to distillate) of 34wt%. Properties of the total liquid products as a function of severity are discussed.

Introduction

In refineries, in order to convert heavy oils and bitumen, it is necessary to subject these materials to thermal treatment to various degrees. In processes where relatively high temperatures are required, solid deposits may be formed as coke that significantly reduces the efficiency of the processing unit. For instance, in the delayed coking operation for processing Athabasca bitumen, the material is heated to temperatures in the range of 350-500°C (1). At these temperatures and in the absence of hydrogen, significant coke deposits can be formed on the walls of furnaces. These deposits currently can be removed by a pigging technique (1). It is believed that petroleum is a colloidal system consisting of asphaltene cores dispersed in solution by a polar fraction, namely resins. During thermal reaction this protective resin layer is destroyed and the asphaltene become exposed. They are no longer soluble in the media, resulting in precipitation and, finally, coke is formed. There are a number of methods and techniques that have been used to measure the stability and fouling tendency of petroleum feedstocks and products:

1. spot test (ASTM-D-4740-95);
2. total sediment (ASTM-4870-96);
3. solubility parameters, optical microscope (2);
4. light scattering (PORLA) (3)
5. peptization value (P-value) (4)
6. colloidal instability index (CII) (5-6);
7. coking index (7).

If the coking onset of petroleum materials can be predicted during thermal processing, it would then be possible to avoid processing severities at which coke formation occurs. Data on the coking onset are also necessary for the design of different processing units. In the present work we adapted solubility parameters, through

an optical microscopy method that was developed by Wiehe (2) to determine the coking onset of Athabasca bitumen.

Experimental

Thermal reactions were performed using a 300 mL autoclave equipped with an insert (sleeve) for ease of removal and transfer of the products after the reaction. Feedstock used in this work was Athabasca bitumen obtained from Newalta, and originating from "Dover SAGD project" (previously UTF) operated by Devon Canada. To perform thermal cracking, about 100 grams of the bitumen was warmed to 40°C and transferred to the autoclave sleeve. The sleeve was inserted into the 300 mL autoclave and the head tightened down using a torque wrench. The autoclave was then purged with nitrogen three times and pressure tested to 550 psi.

The excess pressure was reduced down to 100 psi. The autoclave was then insulated and its content was soaked to 150°C for one hour while stirring. The reactor was heated at 2.5-5°C/min to the final reaction temperature of 370-430°C. The severity index (SI) of the reaction was calculated according to the following equation:

$$SI = t \cdot \exp(-(E_a/R) \cdot (1/T - 1/700))$$

[where t = reaction time, seconds; E_a = activation energy, taken as 50.1 kcal/mole; R = gas constant, 0.001987 kcal/(mole °K); and T = reaction temperature, °K]

Upon achieving the pre-determined severity, the furnace was shut down and the insulation was removed. A cooling purge was directed to the head of the autoclave. The maximum internal temperature, the maximum pressure and the final severity index were recorded.

The autoclave was allowed to cool to room temperature and the gaseous products were collected into a gasbag (Calibrated Instruments Inc.) through a condenser. The condenser was cooled using dry ice to collect the light ends. The volume of the gas in the gasbag was determined by a gasometer with the barometric pressure and temperature recorded at that time. The contents of the gasbag was then analyzed for its components using a gas chromatograph (MTI Quad-series refinery gas analyzer).

The liquid products in the sleeve as well as the small amount of liquid collected in the reactor (as a result of overflow or condensation) were mixed. The light ends that were collected in the condenser were added to this mixture to produce total liquid products (TLP). The material balance (gas and TLP) and pitch conversion are shown in Table 1. The properties of TLP, including solubility numbers and stability index as defined by P-values, are shown in Table 2.

Results and discussion

During thermal treatment of petroleum in the refinery units, a solid deposit or coke is often formed. It has been shown that the coking onset coincides with the insolubility of converted asphaltene (8) due in part to the conversion of resins that protect the asphaltene (7). There is also an induction period for coke formation, which depends on the feedstock and the severity of the process (9). In order to determine the coking onset of Athabasca bitumen, this material was subjected to different severities shown in Table 1. Using high temperature simulated distillation, conversion of +524°C to distillate (pitch conversion) was calculated (Table 1). Up to a severity of almost 5000 seconds, there was no coke (toluene insolubles) formed. At this severity, the pitch conversion was about 34wt%. These results are consistent with our previous data on the visbreaking of Athabasca

bitumen in a continuous bench-scale unit where no coke was formed at a pitch conversion of around 33wt% (10).

The properties of the TLP are shown in Table 2. Although there is some scatter in the data, in general, as the severity of the process increased the heptane asphaltenes (not corrected for the small amount of toluene insolubles) increased. Toluene insolubles (coke) did not increase with severity up to 5000 seconds and examination of TLP under a microscope showed the presence of no solid particles or coke. Again, as expected and accepting the scatter in the data, both MCR and aromaticity increased with severity. A significant reduction in viscosity was observed as the severity increased. The solubility numbers including S_{BN} (solubility blending number) and I_N (insolubility number) as determined by Wiehe's method are shown in Table 2. The P-values, which are indicative of the stability of total liquid products, are calculated from the ratio of S_{BN}/I_N and are also shown in Table 2. As the severity of the process increased the stability of products decreased because the converted asphaltenes became less soluble (higher I_N) and because the solvent quality became slightly poorer (lower S_{BN}). In a previous study (11) it was suggested that by using solubility numbers, it might be possible to predict the onset of coke formation for petroleum feedstocks. In Figure 1, S_{BN} and I_N are plotted against the severity of the process. From the least square straight-line equations obtained for S_{BN} and I_N , it is possible to predict that at a severity index of 7576 seconds asphaltenes will become insoluble ($S_{BN} = I_N$) and start forming coke. To verify, a series of autoclave runs were performed at a relatively high severity, as shown at the bottom of Table 2. Unfortunately, the data from experiments at 6000 and 7000 seconds are not available and will be carried out shortly to better define the coke induction period. Nevertheless, as predicted, all runs of severities higher than 7576 seconds did produce coke. For example, thermal cracking of Athabasca bitumen at a severity of about 8500 produced 4.5wt% coke, and the C7 asphaltenes (not corrected) also increased significantly. It is expected that at the end of the coke induction period (i.e., at the severity where coke starts forming) the asphaltenes concentration will be reduced (8). For this reason the percentage of C7 asphaltenes, after correcting for toluene insolubles, should have been lower than what is reported in Table 2. For the last three runs, at high severities beyond the coke induction period, it was necessary to filter out the solid particles (coke) in order to determine the solubility numbers (S_{BN} and I_N). These solubility numbers do not follow the linear behavior of those within the coke induction period because the least soluble asphaltenes precipitated to form coke.

Conclusions

Thermal reaction of Athabasca bitumen was carried out in a batch autoclave at SI ranging from approximately 500-9500 seconds. It was shown that up to a severity index of around 5000 seconds there was no solid or coke formed. At this severity, pitch conversion was estimated to be about 34wt%. From the solubility numbers of the total liquid products versus the severity, it was possible to predict the onset of coke formation for Athabasca bitumen.

Acknowledgements

Partial funding for NCUT has been provided by the Canadian Program for Energy Research and Development (PERD), the Alberta Research Council (ARC) and the Alberta Energy Research Institute (AERI).

References

- (1) Parker, R. J., and McFarlane, R.A., "Mitigation of fouling in bitumen furnaces by pigging", Proceedings of International conference on petroleum phase behavior and fouling, AIChE Spring National Meeting, Houston, Texas, March 14-18, 1999.
- (2) Wiehe, I.A. and Kennedy, R.I. "The oil compatibility model and crude oil incompatibility", *Energy & Fuels*, 14, 56, 2000.
- (3) Vilhunen J, Alain Quignard, Pilvi O, and Waldvogel, J. "Experience in use of automatic heavy fuel oil stability analyzer", Proceedings of the 7th international conference of stability and handling of liquid fuels, October 13-17, Vancouver, BC., 985-987, 1997.
- (4) Rahimi, P.M., Parker, R.J. and Wiehe, I.A. "Stability of visbroken products obtained from Athabasca bitumen for pipeline transportation", Symposium on heavy oil resid compatibility and stability, 221st ACS National Meeting, San Diego, CA, USA, April 1-5, 2001.
- (5) Gaestel, C., Smadja, R. and Lamminan, K.A. "Contribution a la Connaissance des proprietes des bitumen routiers". *Rev Gen Routes Aerodromes*, 85, 466, 1971
- (6) Asomaning, S.A. and Watkinson, A.P. "Petroleum stability and heteroatoms species effects on fouling heat exchangers by asphaltenes. *Heat Transfer Engng*, 12, 10-16, 2000.
- (7) Schabron, J.F., Pauli, A.T., Rovani Jr., J.F. and Miknis, F.P. "Predicting coke formation tendencies," *Fuel*, 80, 1435-1446, 2001.
- (8) Wiehe, I.A. "A Phase-Separation Kinetic Model for Coke Formation", *I&EC Research*, 32, 2447-2454 (1993).
- (9) Wiehe, I.A. "A Series Reaction, Phase-Separation Kinetic Model for Coke Formation from the Thermolysis of Petroleum Resid, presented at the AIChE Spring Meeting, New Orleans (1996).
- (10) Parker, R. J., Lefebvre, B. and Pipke, A. "Visbreaking of heavy oils for pipeline transportation – quality and stability", presented at the 2nd International conference on petroleum and gas phase behavior and fouling, August 27-31, 2000, Copenhagen, Denmark
- (11) Rahimi, P.M., Parker, R.J., Knoblauch, R. and Wiehe, I.A., "Stability and compatibility of partially upgraded bitumen for pipeline transportation", Proceedings of the 7th International conference on stability and handling fuels, September 22-26, 2000, Graz, Austria, 177-192.

Table 1. Products yields as function of severity

SI, second	Liquid wt%	Gas wt%	Pitch Conv * wt%
	98.1	0.20	5.4
591.97	98.1	0.20	5.4
599.86	98.9	0.04	5.4
708.28	99.2	0.26	5.4
795.31	99.2	0.31	ND
897.92	99.0	0.31	7.3
986.82	99.7	0.3	ND
1095.60	99.1	0.10	9.1
1163.00	98.0	0.3	ND
1445.25	98.1	0.43	14.5
1652.64	98.1	0.47	16.3
1740.50	99.2	0.5	ND
1858.48	99.6	0.51	15.4
2240.71	98.0	0.7	ND
2406.15	98.3	0.52	18.2
2999.42	99.2	0.87	24.5
4319.59	97.4	1.37	32.7
4602.50	98.4	1.29	34.5
5037.33	97.4	1.53	34.5

* Conversion of +524°C to distillate determined by GC simulated distillation

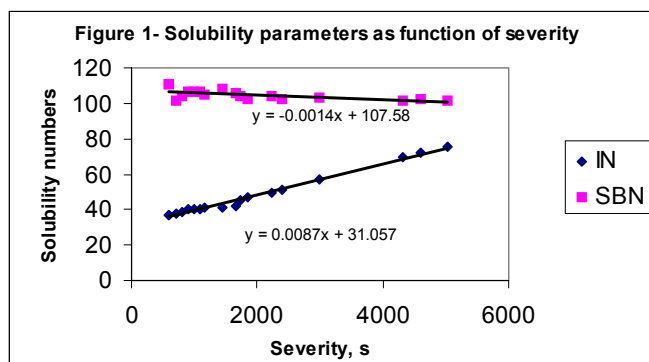
ND = not determined

Table 2. Properties of total liquid products

Severity Index, s	Heptane* Insol wt%	Toluene Insol wt%	MCRT wt%	Aromaticity f_a	Viscosity cP @ 25°C	I_N	S_{BN}	P-value
Bitumen	11.3	0.03	13.7	0.33	174000	33.2	101.5	3.1
592	12.4	0.06	13.4	0.43	54800	37.3	111.0	3.0
600	12.4	0.07	13.0	0.41	57100	37.3	111.0	3.0
708	12.6	0.04	13.2	0.40	46300	38.2	101.5	2.7
795	ND	ND	ND	ND	ND	38.6	104.3	2.7
898	12.4	0.04	12.3	0.38	22000	40.7	106.6	2.6
987	ND	ND	ND	ND	ND	40.7	106.6	2.6
1096	12.7	0.02	13.1	0.39	19700	40.7	106.6	2.6
1163	ND	ND	ND	ND	ND	41.2	104.6	2.5
1445	11.5	0.03	14.2	0.40	11566	41.4	108.5	2.6
1653	12.4	0.11	14.0	0.42	9713	42.1	105.4	2.5
1741	ND	ND	ND	ND	ND	45.3	104.1	2.3
1858	12.5	0.00	13.2	0.45	5810	47.1	102.7	2.2
2241	ND	ND	ND	ND	ND	49.4	103.7	2.1
2406	11.6	0.04	13.9	0.38	3540	51.3	102.5	2.0
2999	12.9	0.04	14.9	0.39	2860	56.8	103.4	1.8
4320	13.6	0.04	15.1	0.40	984	69.4	101.3	1.5
4603	14.0	0.10	15.1	0.42	1686	72.1	102.3	1.4
5037	13.5	0.13	15.4	0.46	750	75.6	101.4	1.3
8564	18.95	4.55				102.5	114.8	1.12
9454	16.42	4.58				89.4	109.1	1.22
9692	17.61	5.94				102.2	112.2	1.1

* Including Toluene insolubles

ND = not determined



HYDROCRACKING OF ASPHALTENES WITH METAL CATALYSTS SUPPORTED ON MESOPOROUS SILICA

Enkhsaruul Byambajav, Ryozo Tanaka,¹⁾ Yasuo Ohtsuka

Institute of Multidisciplinary Research for Advanced Materials, Tohoku University, Katahira, Aoba-ku, Sendai 980-8577, Japan

¹⁾Central Research Laboratories, Idemitsu Kosan Co., Ltd., Kamiizumi, Sodegaura, Chiba 299-0293, Japan

Introduction

Heavy oils contain significant amounts of asphaltenes, which are frequently responsible for catalyst deactivation in the upgrading processes. To produce lighter distillates efficiently from heavy oils, it may be necessary to better understand the chemistry of asphaltene cracking in the reaction space suitable for the molecules.

Since the molecular size of asphaltene aggregates is known to range more than 2 nm¹⁾, the present authors have been working on the utilization of mesoporous silica materials with pore diameters of 2 – 30 nm as catalyst supports for asphaltene cracking. When iron catalysts are loaded on mesoporous silica (SBA-15²⁾) supports with different pore diameters, asphaltene conversion during cracking at 573 K increases with increasing average pore diameter up to 12 nm but levels off beyond this value, regardless of the absence and presence of pressurized H₂³⁾. In this work, therefore, SBA-15 support with the pore diameter of 12 nm is used as a catalyst support, and the effects of metal type, loading and kind of asphaltene on the cracking performance in pressurized H₂ are examined.

Experimental

SBA-15 was synthesized by heating an acidic aqueous mixture of triblock copolymer (EO₂₀PO₇₀EO₂₀), trimethylbenzene, and TEOS at 308 K for 24 h, followed by post-synthesis heat treatment at 370 K²⁾,⁴⁾. The material recovered after filtration and subsequent dryness at room temperature was calcined in air at 773 K for 6 h. Fe or Ni catalyst was loaded on SBA-15 support by the impregnation method using an ethanol solution of Fe(NO₃)₃ or Ni(NO₃)₂, respectively, and the resulting sample was again air-calcined at 773 K, metal loading being 10 wt%, unless otherwise stated. All of catalysts were subjected to N₂ adsorption and X-ray diffraction (XRD) measurements. The pore size distribution and specific surface area were determined by the BJH and BET methods, respectively.

Asphaltene (soluble in toluene but insoluble in n-heptane), separated from vacuum residue of crude oil from the Middle East, was mainly used in this study. The elemental analysis is: C, 84.0; H, 7.8; N 0.9; S, 5.3, O (by difference) 2.0 wt%. Other asphaltenes from difference sources were also used. A toluene solution of asphaltene with a concentration of 100 mg/l was mixed with catalyst under ultrasonic irradiation, weight ratio of asphaltene and catalyst being 1.0. The resulting mixture was then evacuated at room temperature with a rotary evaporator to remove toluene, followed by dryness at 363 K under vacuum.

Cracking runs in pressurized H₂ at 5.0 MPa were carried out at 573 K for 1 h with a stirred autoclave. Solid products were separated by the Soxhlet method using n-heptane and toluene into maltene (heptane-soluble), recovered asphaltene (toluene-soluble), and coke plus catalyst (toluene-insoluble). The temperature programmed oxidation (TPO) of the latter mixture recovered was performed, and SO₂ evolved was on line determined.

Results and Discussion

Catalyst Properties and Structures. Figure 1 shows typical examples for the pore size distribution of SBA-15 support and fresh

Fe/SBA-15 catalysts after air calcination. All of the materials used provided the narrow distribution with a sharp peak at pore diameter of about 10 nm. When the Fe was added to the support, the peak height decreased with increasing Fe loading, which means that Fe oxide particles are held inside the mesopores. Pore properties and XRD results are summarized in Table 1. The SBA-15 support had the average pore diameter of 12 nm, pore volume of 2.6 cm³/g and BET surface area of 790 m²/g. Catalyst addition did not change the pore diameter, irrespective of metal type and loading, but lowered the pore volume and surface area, as is expectable. The extent of the lowering was larger at a higher loading.

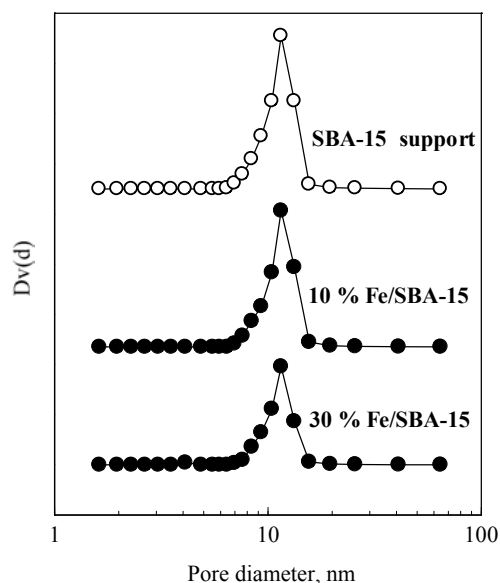


Figure 1. Pore size distribution of SBA-15 support and Fe/SBA-15 catalysts after air calcination.

Table 1. Properties of Metal Catalysts Supported on SBA-15

Metal	D _p ¹⁾ (nm)	V _p ¹⁾ (cm ³ /g)	S _{BET} ²⁾ (m ² /g)	XRD species
None	12	2.6	790	-
10 wt% Fe	12	2.3	680	n.d. ³⁾
30 wt% Fe	12	1.5	520	n.d. ³⁾
10 wt% Ni	12	2.1	620	NiO

¹⁾Average pore diameter (D_p) and pore volume (V_p).

²⁾BET surface area.

³⁾No species detectable.

As is seen in Table 1, the XRD measurements of the fresh catalysts revealed that no significant diffraction lines of Fe oxides were detectable, independently of Fe loading, whereas NiO peaks appeared with 10 % Ni/SBA-15. The average crystalline size of NiO determined by the Debye-Scherrer method was estimated to 8.0 nm, which was smaller than the average pore diameter (12 nm) of the Ni/SBA-15. These observations suggest that Fe species are more finely dispersed inside the mesopores than Ni species.

Hydrocracking Performances and Catalyst Forms. The results for hydrocracking at 573 K are shown in Figure 2, where asphaltene conversion and maltene yield are calculated by using the amounts of asphaltene and maltene recovered, respectively. With Fe catalysts, interestingly, the conversion was the highest at 4 % Fe and

decreased with increasing Fe loading, whereas maltene yield was the largest at 10 % Fe. It is evident that the optimum Fe loading exists for maltene formation. The 10 % Ni catalyst showed the lower conversion but the higher yield than the 10 % Fe catalyst. The latter may originate from higher hydrogenation ability of the Ni.

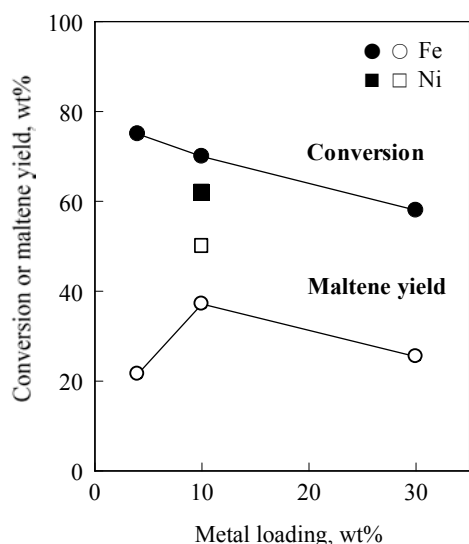


Figure 2. Asphaltene conversion and maltene yield in hydrocracking with Fe/SBA-15 and Ni/SBA-15 catalysts.

The XRD profiles after reaction showed that any Fe species could not be detected with 4 – 10 % Fe catalysts, but very small peaks of Fe_3O_4 were observed at 30 % Fe. The NiO observed with the fresh Ni/SBA-15 was reduced partly to metallic Ni after reaction.

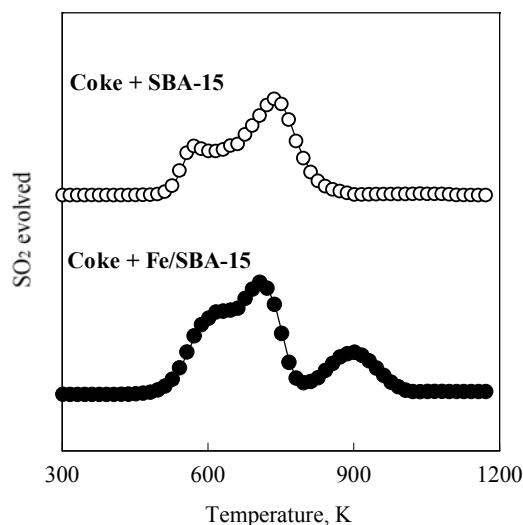


Figure 3. TPO profiles for the mixture of coke and SBA-15 support or 10 % Fe/SBA-15 catalyst recovered after reaction.

To examine the surface state of the 10 % Fe catalyst used, the TPO runs were carried out. The results are shown in Figure 3. When the profiles without and with the Fe catalyst were compared, SO_2 evolved newly at 900 K in the presence of the Fe. The SO_2 can be ascribed to the decomposition of FeSO_4 ⁵⁾, which arises probably

from the oxidation of surface iron sulfides during the TPO. The elemental analysis revealed that most of the sulfur evolved during asphaltene cracking was retained in the mixture of coke and Fe/SBA-15 or Ni/SBA-15 catalyst. It is likely that Fe and Ni catalysts are present in the sulfided forms at the outermost layers.

From these observations, following speculations are possible for the optimum Fe loading for maltene formation observed in Figure 2. The sulfide species at 4 % Fe are the most highly dispersed and thus show the largest catalytic activity, which results in the highest coke yield. At 10 % Fe, on the other hand, fine particles with the larger size than that at 4 % Fe exist and show the medium activity and largest hydrogenation ability for maltene formation.

When two kinds of asphaltenes derived from different vacuum residues from the above-mentioned were cracked with the 10 % Fe/SBA-15, asphaltene conversion and maltene yield depended on its type, and the highest conversion reached about 80 %, which was larger than the value in Figure 2. Although atomic H/C ratios in all of feed asphaltenes used were almost the same, the XRD measurements revealed the different compositions of aliphatic and aromatic fractions observed at $2\theta(\text{Cu K}\alpha)$ of 20 – 22 and 25 degrees⁶⁾, respectively. The proportion of the latter fraction seems to relate with the extent of coke formation.

Conclusions

Mesoporous silica (SBA-15) with narrow pore size distribution and average pore diameter of 12 nm is synthesized and used as a support of Fe or Ni catalyst in hydrocracking of asphaltenes at 573 K and under 5.0 MPa H_2 . When Fe loading is changed in the range of 4 – 30 wt%, asphaltene conversion is higher at a smaller loading, and maltene yield is the largest at 10 % Fe. The 10 % Ni/SBA-15 shows the lower conversion but the higher yield than the 10 % Fe catalyst. The elemental analysis and temperature programmed oxidation show that most of sulfur evolved during hydrocracking is retained in the mixture of coke and catalyst, and the catalyst surface exists in the sulfided species, which are probably active for asphaltene cracking.

Acknowledgement. This work was carried out in part as a research project of the Japan Petroleum Institute commissioned by the Japan Cooperation Center, Petroleum, with the subsidy of the Ministry of Economy, Trade and Industry.

References

- (1) Yen, T. F. In *Encyclopedia of Polymer Science and Engineering*; Grayson, M.; Krochwitz, J.L., Eds.; Wiley: New York, 1988; p.1.
- (2) Zhao, E.; Feng, J.; Huo, Q.; Melosh, N.; Fredrickson, G.; Chmelka, B.; Stucky, G. *Science* **1998**, *279*, 548.
- (3) Byambajav E.; Ohtsuka, Y. Proc., 52nd Canadian Chemical Engineering Conference, No. 405 (2002).
- (4) Wang, Y.; Noguchi, M.; Takahashi, Y.; Ohtsuka, Y. *Catal. Today* **2001**, *68*, 3.
- (5) LaCount, R. B.; Anderson, R. R.; Friedman, S.; Blaustein, B. D. *Fuel* **1987**, *66*, 909.
- (6) Scotti, R.; Montanari, L. In *Structure and Dynamics of Asphaltenes*; Mullins O.C.; Sheu, E.Y., Eds.; Plenum Press: New York, 1998; p.79.

MOLECULAR CONSTITUTION, CARBONIZATION REACTIVITY, AND MESOPHASE DEVELOPMENT FROM FCC DECANT OILS

Jennifer Clemons, Guohua Wang and Semih Eser

Dept of Energy and Geo-Environmental Engineering/
Energy Institute

The Pennsylvania State University, 101 Hosler Building, PA 16802

Introduction

FCC (Fluidized Catalytic Cracking) decant oils are the primary feedstock to the delayed coker to produce highly graphitizable precursor—the needle coke. The quality of needle coke is determined, in essence, by the development of mesophase formation in the early stages of liquid-phase carbonization that, in turn, closely relates to the chemical composition, carbonization reactivity of coker feedstock, sulfur content and coking conditions [1,2,3].

The objective of this study was to investigate the effects of molecular composition and the reactivity of blending streams in coker feedstock on the mesophase development and needle coke texture.

Experimental

Coker Feedstocks. The samples used in this study come from a commercial needle coke plant. They include virgin decant oil, gas oils, hydrotreated decant oil stream and coker charge.

Carbonization Experiment. Carbonization experiments were conducted in tubing bomb reactors (15 mL) at 500°C for 3 hours under autogenous pressure. The reactors were heated in a fluidized-sand bath. After reaction, the reactors were quenched in cold water. The semi-coke product was recovered as whole piece for microscopic examination. For the study of reactivity of sample effects on the mesophase development, the sample was heated at 450°C from 20 minutes up to 5 hours in the same isothermal sand bath. The yields of semi-coke (defined as dichloromethane insoluble) and asphaltene (pentane soluble and dichloromethane insoluble) were determined by sequential solvent extraction.

Coker feedstock molecular analyses. Gas Chromatography with Mass Spectrometer (GC/MS, Shimadzu GC-17A, MS-OP-5000), High Performance Liquid Chromatography with Photodiode Array detector (HPLC/PDA), Laser Desorption with Mass Spectrometer (MALDI-TOF-MS) and Liquid Chromatography with dual mass spectrometers (LC/MS/MS) were used to characterize the samples.

Semi-coke optical texture. The extent of mesophase development in the liquid-phase carbonization of samples was measured quantitatively in terms of Optical Texture Index (OTI). Each semi-coke sample was mounted in a pellet of epoxy resin, then cut into two sections. The polished pellets were examined under a polarized light microscope (Nikon-Microphoto_FXAI). We used a 1.1 mm X 1.1 mm mask and 10X object lens to acquire the surface images. At least 250 images were examined for a pellet. The OTI of semi-coke was determined according to following equation [4]:

$OTI = \sum f_i * OTI_i$ where f_i is the numerical fraction of individual texture types from microscopic analysis and OTI_i is the index value assigned to each texture type, as defined in Table 1.

Table 1. Index Assignments for OTI definition to characterize optical textures of semi-coke samples.

Type	Size/Shape	Index (OTI)
Mosaic	<10 μm	1
Small Domain	10-60 μm	5
Domain	>60 μm	50
Flow Domain	>60 μm long, >10 μm wide	100

Results and Discussion

OTIs of semi-coke samples produced at 500°C for 3 hours are listed in Table 2. We see a significant variation among the degree of mesophase development in the sets of coker feedstock samples. DO02-1 produced a semi-coke with much lower extent of mesophase development while DO02-4 produced more anisotropic coke with high proportion of flow domain texture. Coker charges of both decant oils give a better mesophase development than their parent decant oils, the heavy stream (VTB) of DO02-4 produced even more anisotropic coke (88 of OTI).

Table 2. OTI of semi-coke samples from coker feedstocks.

	Flow Domain	Domain	Small Domain	OTI
CF02-1	54	58	5	71
CF02-4	74	31	0	85
DO02-1	68	89	7	69
DO02-4	77	38	0	83
VTB 02-4	105	35	0	88

Decant oil 02-1 and 02-4 have different major hydrocarbon distributions: as GC/MS quantitative results show (Figure 1 and Figure 2), there is much less pyrene and alkylated pyrenes present in DO02-1 than in DO02-4; normal alkanes concentration in DO02-1 is about two times higher than in DO02-4. Both Coker feeds have higher concentration of phenanthrenes and pyrenes, and lower concentration of normal alkanes than their parent decant oils. The variations in hydrocarbon compositions show similar trends as those noted for the corresponding decant oil samples.

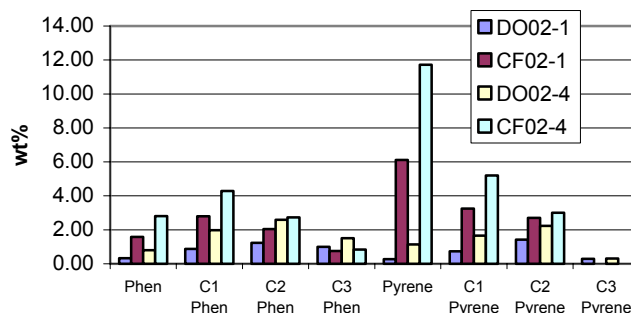


Figure 1. Aromatic compound distribution in feedstock samples.

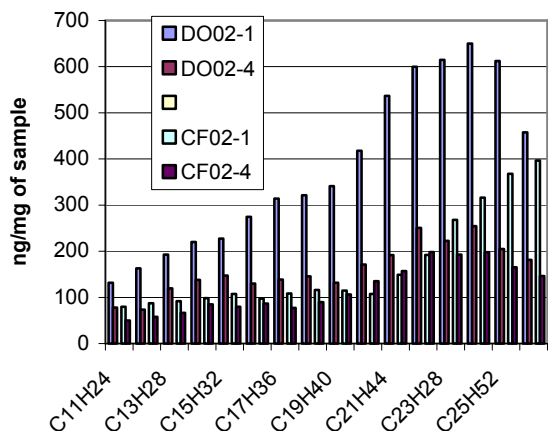


Figure 2. Aliphatic compound distribution in feedstocks.

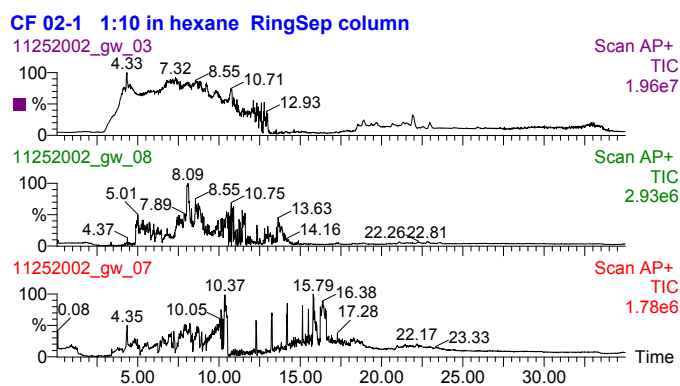


Figure 3. LC/MS/MS chromatograms of CF02-1 (Top), CF02-4 (Middle) and VTB02-4 (Bottom).

Differences in heavier hydrocarbon compound constitution are clearly seen on the TIC of LC/MS/MS chromatograms. We see the higher aliphatic contribution to the TIC in the initial region (retention time from 3 to 8 minutes) in sample CF02-1. In the five- to six- ring aromatic region (about 13min to 17min), the molecular constitution in CF02-4 is much simpler than in CF02-1. Major aromatic compounds include the trimethyl-, tetramethyl and pentamethyl-benzopyrene and benzoperylenes. Note the relatively high intensity peaks in the longer retention time region (20min to 25min) in CF02-1. These are the alkylated (up to C3) benzocarbazoles. In VTB sample, the heavy aromatic compounds almost exclusively consist of C1 to C4 benzopyrene and benzoperylenes (Figure 3, bottom).

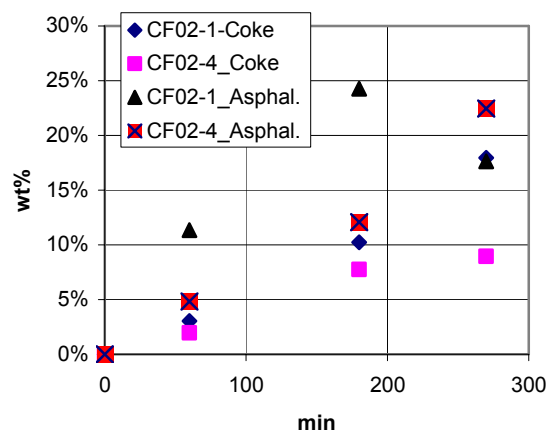


Figure 4. Coke and asphaltene yields of coker feeds

Intermediate (asphaltenes) and solid coke product yields from coking experiments (450°C) are presented in Figure 4. By comparing sample CF02-1 with CF02-4, the rapid build-up (within 180 minutes) in asphaltenes in CF02-1 indicated the high reactivity of compounds in this coker feed. The short time window in the case of CF02-1 for the mesogens to stack and grow into large mesophase sphere and form elongated flow domain may explain the lower anisotropy of the semi-coke produced. The difference of reactivity between these two samples is consistent with their molecular composition difference: CF02-1 contains a higher concentration of normal-alkanes than CF02-4. Alkanes are the least thermally stable compounds in the carbonization environment that easily crack to form free radicals to serve as polymerization initiators. Higher concentration of alkanes in coker feed would result in a higher rate of carbonization that would lead to a lower degree of anisotropy in the semi-coke texture.

Conclusions

Differences in molecular composition of FCC decant oils and coker feeds derived from decant oils can be related to the differences obtained in the degree of mesophase development obtained upon carbonization of these materials. Concentration of n-alkanes, and the distribution of PAH in the coker feeds affect the rate of coke formation and, thus, the extent mesophase development.

Acknowledgement. Financial support from Chicago Carbon Company and many helpful discussions with Robert Miller of Chicago Carbon Company are gratefully acknowledged.

References

- (1) Eser, S. in Supercarbon: Synthesis, Properties and Applications, ed. By Yoshimura, S. and Chang, R.P.H., Springer-Verlag, Berlin, 1998, p147.
- (2) Mochida, I., Fujimoto, K. and Oyama, T. in Chemistry and Physics of Carbon, Vol 24, ed. By Thrower, P. A., Marcel Dekker Inc., New York, 1994, p111.
- (3) Filley, R.M. and Eser, S., Energy & Fuels, 1997, 11, 623.
- (4) Yang, M-G, Wang, G. and Eser, S., Eurocarbon 2000, International Conference on Carbon, pp. 163-164.

BIOCONVERSION OF AROMATICS IN LIGHT GAS OIL (LGO) IN A CONTINUOUS BIOREACTOR SYSTEM

Hans Kr. Kotlar¹, Kjetil Rasmussen², Knut Grande¹, Marit Ramstad²,
Sidsel Markussen², Asgeir Winnberg², Sergey Zotchev³
and Martin Gimmestad³

¹ Statoil R&D, Trondheim

² SINTEF Applied Chemistry, Trondheim

³ Department of Biotechnology, NTNU

Introduction

The content of polyaromatic hydrocarbons (PAH's) in the diesel fuels contribute to low cetane numbers and particle emissions from combustion.

The present paper focuses on the use of a continuous bioreactor system for upgrading of the LGO as a potential industrial process. This is done by biocatalytic ring opening of the PAH's to generate a more paraffinnic diesel fuel.

Two different bacterial strains, *Sphingomonas yanoikuyae* DSMZ 6900 N2 and *Pseudomonas. fluorescens* LP6a 21-41 (donated by Dr. Julia Foght, University of Edmonton Canada), were compared for biocatalysis of the PAH's in the LGO feed stock from the refinery.

S. yanoikuyae was found to have all the enzymes necessary for the desired bioconversion. The PAH degradation pathway was genetically engineered in order to obtain a recombinant strain accumulating one of the precursors, 2-hydroxychromene-2-carboxylate. This could be achieved by eliminating the enzyme activity for the specific hydratase-aldolase (NahE) responsible for further degradation of 2-hydroxychromene-2-carboxylate. Thus, the degradation of PAH would terminate after the ring opening, which is important for keeping the octane number of the hydrocarbon fraction. The strategy chosen was to inactivate the gene encoding NahE by gene disruption. Five mutants with an inactive nahE gene have been constructed, and the N2 mutant was chosen for further investigation.

P. fluorescens LP6a has been obtained by transposon mutagenesis, and its genetic background remained unknown.

Results & Discussion

A toxicity test of LGO on both N2 and LP6a 21-41 was performed. Figure 1 shows the growth curves of both strains in a yeast extract (YE) based medium and medium with 50 % LGO. No inhibitory effects were observed. However, color change of the suspensions containing LGO strongly indicated conversion of LGO components. In addition, the color of the N2 suspension turned red while the LP6a developed a yellow color indicating a difference in the composition of converted LGO-components. These observations suggested that the two strains had different affinities for different hydrocarbons and that there may be a substrate competition for the active sites of the enzyme systems.

Since the LGO did not inhibit growth of either of the strains, a continuous feed of 20 vol % was used in the experiments on bioconversion. However, LP6a and N2 cells clearly differed in their ability to degrade PAH, since different colored intermediates were produced upon incubation of their suspensions with LGO.

Toxicity test of LGO on N2 and LP6a 21-41

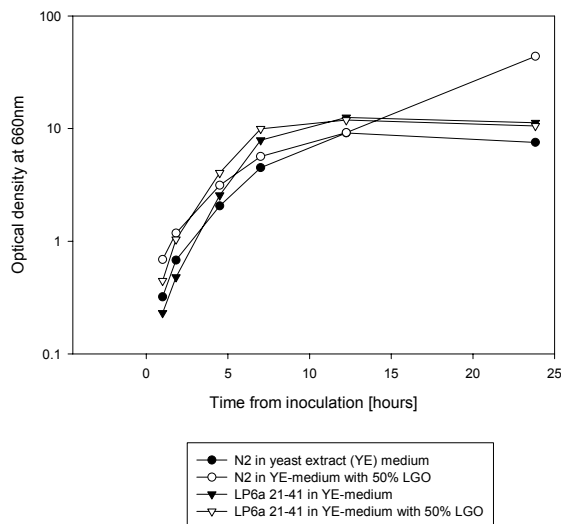


Figure 1. Toxicity testing of LGO on the N2 and LP6a strains

LP6a and N2 were also compared in a PAH degradation assay utilizing dibenzothiophene (DBT) as a main substrate with selective addition of naphthalene, benzene and toluene. Both strains were grown in YE-medium and induced with salicylic acid before harvesting. Equal amount of cells were then transferred to shaker flasks containing 100 ml mineral medium and 0.05 dibenzothiophene (DBT) dissolved in 10 ml hexadecane. The end product of DBT creates a red color absorbing at 475 nm. After two hours benzene, toluene, and naphthalene was added to separate flasks. Figure 2 shows the bioconversion of DBT by the two strains and the effect of adding different aromates. All the added aromates seemed to compete with DBT for the enzyme system of LP6a 21-41. The N2 strain had evidently a higher affinity for naphthalene than DBT, whilst benzene and toluene seemed less attractive.

The results of these experiments confirmed that substrate competition observed for the two cell suspension differed significantly, suggesting different preferences of the two strains for certain PAHs.

Substrate competition - N2 and LP6a 21-41
 Addition of 500 μ l Benzene; 500 μ l Toluene; 0,5g Naphthalene

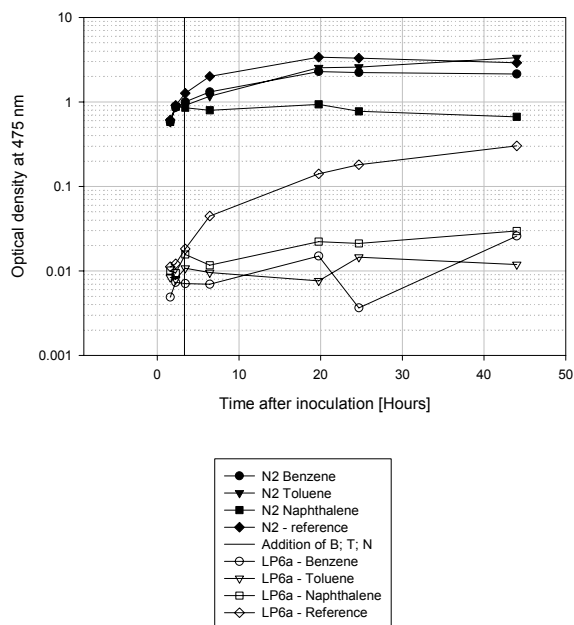


Figure 2. Substrate competition differences between the N2 and LP6a strains

Figure 3 shows the degree of bioconversion of LGO components from a bioreactor run in batch mode with N2. Cells were grown in YE-medium and induced with salicylic acid. Harvested cells were transferred to the bioreactor containing mineral medium and 20% LGO. The results shown in figure 3 indicate that the N2 strain has the highest bioconversion of the least substituted aromates and optimal residence time for the cells in the bioreactor at around 8 hours.

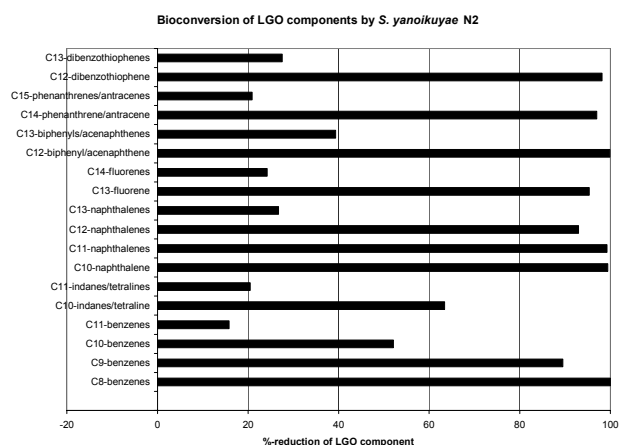


Figure 3. Bioconversion of light gas oil components

In an expanded reactor system the N2 strain will also be grown in a continuous feed bioreactor on oil. Our data suggest, that instead of energy-expensive distillation processes, bioreactor systems have the potential for upgrading of hydrocarbon refinery fractions.